2018

A unified Method For The Design Of Circular Bolted Flange Plate Connections

Pratima Chitrakar
University of Alabama at Birmingham

A UNIFIED METHOD FOR THE DESIGN OF CIRCULAR BOLTED FLANGE PLATE CONNECTIONS

by

PRATIMA CHITRAKAR

FOUAD H. FOUAD, COMMITTEE CHAIR
BO DOWSWELL
NASIM UDDIN

A THESIS

Submitted to the graduate faculty of The University of Alabama at Birmingham,
in partial fulfillment of the requirements for the degree of
Master of Science

BIRMINGHAM, ALABAMA

2018

A UNIFIED METHOD FOR THE DESIGN OF CIRCULAR BOLTED FLANGE PLATE CONNECTIONS

PRATIMA CHITRAKAR

MASTER OF SCIENCE IN CIVIL ENGINEERING

ABSTRACT

The use of steel tubular structures for transmission and distribution poles is increasing widely in the U.S as they are easy to construct and install, require less land space and has aesthetic benefits. In these steel tubular structures, the use of bolted flange plate connection is common. The bolted flange-plate connection is used to connect tubular element and transfer load from one element to the other and then to the foundation. The size and thickness of flange-plate connection depend on the applied loads, number of bolts and material type. For the industrial manufacturing purpose, the simplified and unified design method for circular bolted flange-plate connection is not documented properly. Many investigations focused on the design of flange-plate due to axial load only or due to bending moment only, while some on the effect of prying action.

The objective of this study is to propose a unified simplified design steps for unstiffened circular bolted flange-plate connections integrating the studies done and methods proposed in the past. A detailed study of literature on circular bolted flange plate was done. From integrating the steps of three papers, a complete design steps mitigating the limitations of past analytical methods was proposed. A theoretical parametric study was conducted to study the behavior of connections due to variable parameters. To support the analysis of the theoretical parametric study, FEA analysis was done and it showed similar results as the theoretical parametric study. Furthermore, since this study was based on the results of research work done in the past, the results of the proposed method

was compared with the three methods that were considered while proposing simplified design steps. To verify the results of the proposed method, FEA analysis was done and the results were in good agreement with the theoretical results. This study combine previous design steps and bring together the conclusions eliminating the limitations of the present studies.

DEDICATION

I would like to dedicate this work to my father Prem Bahadur Chitrakar and my mother Mina Chitrakar, who have always loved me unconditionally and whose advice, motivation, and support helped me to work hard for the things I aspire to achieve. I would like to acknowledge my husband Anup Chitrakar, my brother Pradip Chitrakar, my sister-in-law Sanjeela Chitrakar for their love and support.

ACKNOWLEDGMENTS

I would like to express my gratitude to:

- Dr. Fouad H. Fouad, Professor and Chairman of the Civil, Construction, and Environmental Engineering Department, University of Alabama at Birmingham,
- Dr. Bo Dowswell, Adjunct Professor, Civil, Construction, and Environmental Engineering Department, University of Alabama at Birmingham,
- Dr. Nassim Uddin, Professor, Civil, Construction, and Environmental Engineering Department, University of Alabama at Birmingham.

For their support and guidance throughout this research.

TABLE OF CONTENTS

LIST OF TABLES

LIST OF FIGURES

LIST OF ABBREVIATIONS

CHS	Circular Hollow Section
FEA	Finite Element Analysis
RHS	Rectangular Hollow Section
ANSYS	Analysis System
CAD	Computer-Aided Design
TIA	Telecommunications Industry Association
M	Bending Moment that Connections Should Transfer
M_{tube}	Bending Capacity of Tube
M_u	Pole Resultant Overturning Moment Reaction
N	Tensile Force Bolt Should Transfer
Ru	Pole Vertical Reaction
N_{max}	Maximum Tensile Force of Bolts
N^b_t	Design Value of Bolt Tensile Capacity
Tn	Bolt Preload
B	Bolt Force
Q	Prying Force
f, f_{yf}	Flange-Plate Design Yield Strength
n	Number of Bolts
D_t	Diameter of Tube
R	Radius of Tube

D_f	Diameter of Flange-plate
t, t_f	Flange-Plate Thickness
D_{bc}	Diameter of Bolt Circle
a	Distance Between Flange-Plate and Bolt Circle
b	Distance Between Bolt Circle and Tube
γ	Tensile Capacity Index
α	Moment Ratio Factor

CHAPTER 1

INTRODUCTION

1.1 General

Steel tubular structures with its unique advantages like convenience in construction, less land space occupation, aesthetic merit and unambiguous force transfer are widely used for transmission and distribution poles as shown in Figure 1. For splicing steel tubular structures, bolted flange plate connection is considered one of practical solutions. The combination of the circular hollow tube and the circular flange-plate connections with bolts are shown in Figure 2. Besides experiments, many investigations including theoretical study and numerical simulation have been done in the past for flange-plate connection. To verify related design codes for flange-plate connections, an experimental investigation on 63 specimens of unstiffened connections for Circular Hollow Section(CHS) (Kato B, Hirose R, 1985). In the theoretical study, typically T-stub analysis and yield line theory are used to develop suitable design models (Kato B, Mukai A, 1985) (Igarashi S, Wakiyama K, Inoue K, Matsumoto T, Murase Y, 1985) (Packer JA, Bruno L, Pirkemoe PC, 1989) (Cao JJ, Packer JA, Yang GJ, 1998). The behavior of flange-plate connections under bending, prying action, or axial load was studied. These studies have given a strong foundation for further research and study. However, for practical application, simplified design steps need to be put forward.

Figure 1. Tubular steel distribution pole

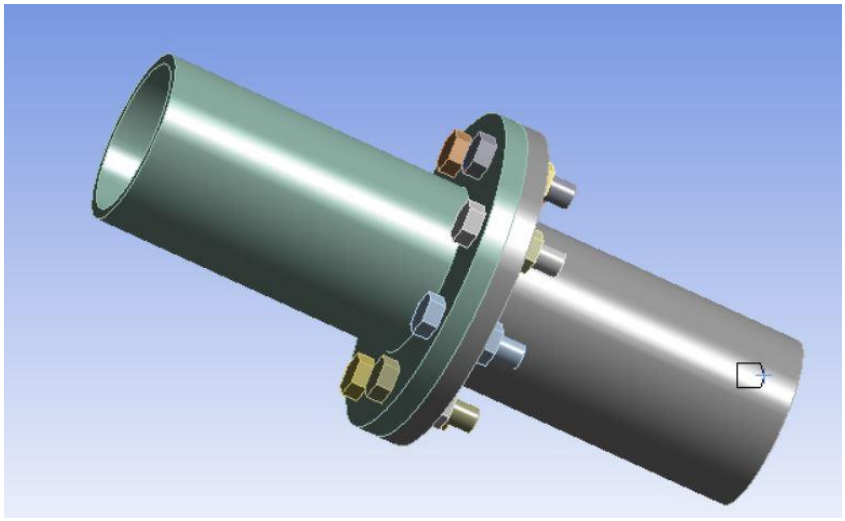

Figure 2. Tubular poles connected by bolted flange-plate

1.1.1 Method of Analysis:

There are two methods of analysis, elastic design, and plastic design. For the load and resistance factor, design of steel structures in the ultimate load criteria, the plastic analysis is used. When the structure resists the applied load continuously till it yields, it is

known as the plastic condition. The stress-strain curve for mild steel and idealized stress-strain response for plastic analysis is shown in Figure 3.

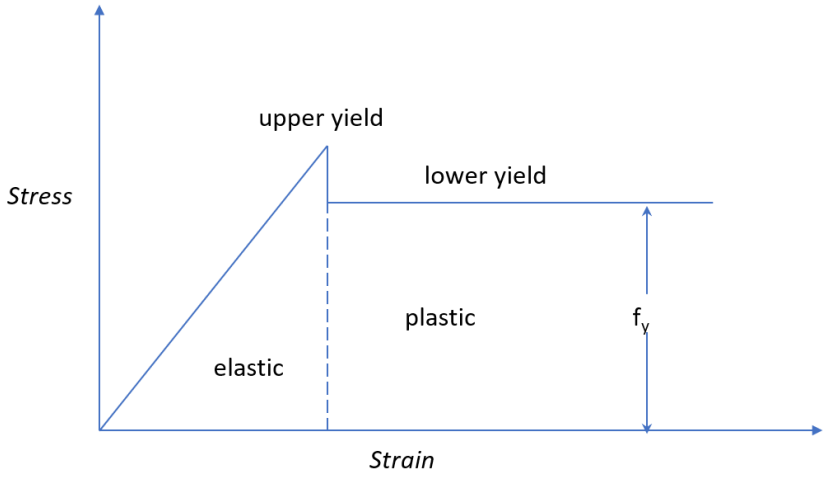

Figure 3. Idealized stress-strain curve in plastic theory

At ultimate load, plastic hinge is formed in the flange-plate connection or on the tube member. Plastic hinge is the section where the structure has reached the yield stress and it will keep deforming without additional load. The formation of plastic hinges either in the joint or in the member is based on the strength of the joints and consequently, it decides the collapse mechanism. If the hinge is to be developed at the joint, then the joint should be detailed with adequate ductility to resist rotation. The basic assumptions of the plastic theory of analysis are as follows:

a) The material shows a lower yield point and can undergo considerable strain without any increase in the stress as shown in Figure 3.

b) The plane section before bending remains plane even after bending.

c) The relationship between compressive stress and compressive strain is same as that of tensile stress and tensile strain.

d) When the fully plastic moment is attained at a section, a plastic hinge is formed, which can undergo the rotation of any magnitude.

e) Effect of shear force on the plastic moment capacity is neglected.

f) The deflections are considered so small that the equations of static equilibrium hold good as if its undeformed structures.

1.1.2 Failure Cases:

The cross-section of T-shape connection is about like the circular tubular flange connection. There are three typical failure cases of T-shape connections as shown in Figure 4 (Fenghua Huang, Dachang Zhang, Wan Hong, Buhuli Li, 2017).

a) When the flange plate is relatively thick, the bending deformation of the flange plate is small, and the bolts are pulled off as shown in Figure 4 (a). In this case, the bolts have achieved the ultimate stress while the flange plate remains in elastic condition. Prying action does not exist in this mode of failure.

b) When the deformation of the flange plate is equal to that of the bolts, a plastic hinge is formed at the weld line and the bolts are pulled to failure as shown in Figure 4 (b).

c) When the flange plate is relatively thin, the deformation of flange plate is larger than that of the bolts as shown in Mode 1 b) Mode 2

c) Mode 3

d) Figure 4(c). The plastic hinge is formed at the flange plate both at the weld line and bolt line and in this mode, flange plate bends in parabola while no bolts yield.

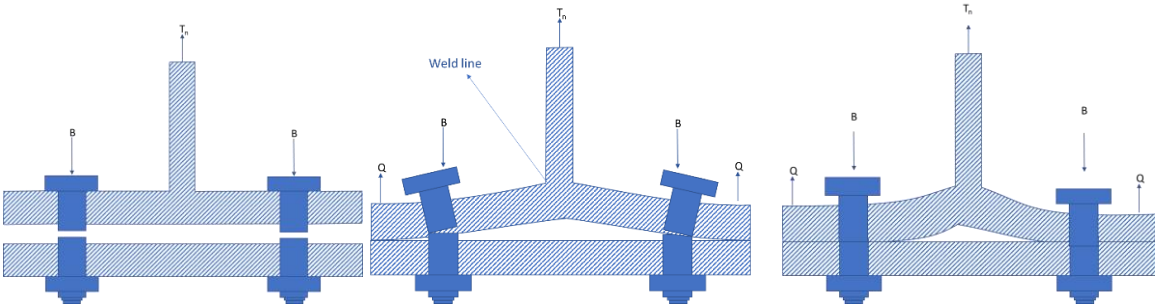

e) Mode 1 b) Mode 2 c) Mode 3

Figure 4. The three failure modes of T-shape connection

1.1.3 Yield Line Method of Analysis:

Yield line method of analysis is a simple and efficient method of calculating the collapse load of relatively thin plates of rigid-perfectly plastic material. Yield lines develop when the rupture gradually increases. Yield lines are the lines of maximum yielding and in the case of unstiffened circular bolted flange plate connections, the yield lines are assumed to develop at the outer diameter of tube and the bolt circle.

1.1.4 Prying Action:

Prying action is a phenomenon that occurs in bolted tension-type connections whereby the deformation of a connecting element under a tensile force increases the tensile force in the bolt. When the bolts are subjected to tension, the center line of bolts acts as a hinge and the tensile force pushes the plate between bolts in the upward direction and pushes the edge part of the plate outside bolt in the downward direction as

shown in Figure 5. The phenomena of plates to push downwards is known as prying action. The force required to resist this action is known as prying force. The additional prying force is added to the applied load to give total bolt force. The prying action can be seen more in the unstiffened connections than in the stiffened connections. As stiffeners share part of the tensile load, prying action is less in the stiffened connections.

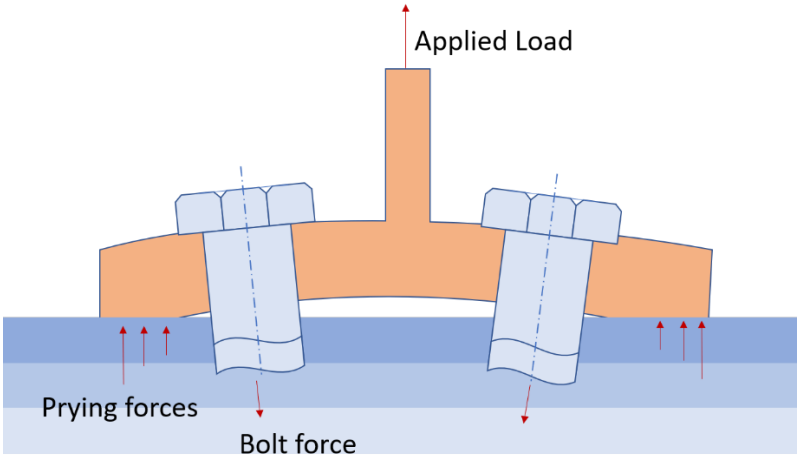

Figure 5. Total force on Bolt

1.1.5 Notations:

The symbols that are used in the calculations are explained here.

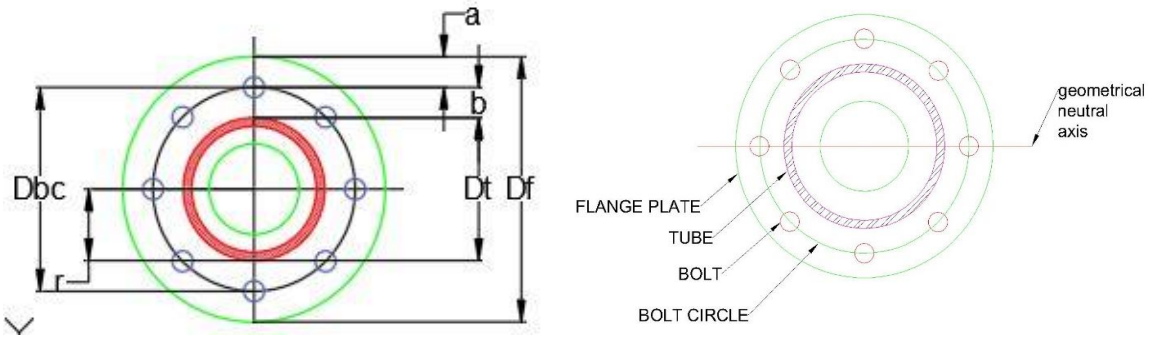

Figure 6. Top view of structural elements of poles

As shown in Figure 6, D_t is the diameter of tube, D_f is the diameter of the flange-plate, D_{bc} is the diameter of the bolt circle, a is the distance between the flange-plate and the bolt circle, and b is the distance between the bolt circle and the outer tube.

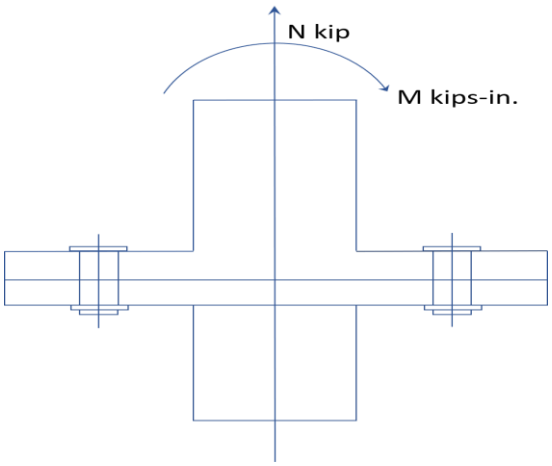

Figure 7. Applied Loads

The applied load arrangement in the poles are shown in Figure 7. Here, N is the axial tensile load and M is the bending moment. This study checks the connections for tensile load and bending moment load only. It is assumed that if the connection is safe in tensile, then it will be safe in compression as well. N_{max}, maximum tensile loads on bolts are computed from the applied loads, N_t^b is the design tensile bolt load.

1.2 Problem Statement

Many experiments and investigations on the behavior of flange-plate connections under axial loading and bending moment have been done. Each research study on bolted flange-plate connections addressed specific topic. The topics are 1) the behavior of joints subjected to bending moment and axial load (Mael Cauchaux, Mohammed Hijaj, Ivor

Ryan, Alain Bureau, 2011) 2) the mechanism and calculation theory of prying force (Fenghua Huang, Dachang Zhang, Wan Hong, Buhuli Li, 2017) 3) the effect of flange geometry on the strength of bolted joints (G M PinFold, 1994). All these research studies and investigations provide foundation and basis to expand knowledge on the bolted flange-plate connections. Based on the experimental results, the behavior of unstiffened and stiffened RHS and CHS are presented and the algorithm for its design is proposed (Y.Q. Wang, L. Zong, Y.J. Shi, 2013). However, for practical construction purpose, unified simplified design steps for unstiffened circular bolted flange-plate connections including flange-plate design and calculation of bolt force including prying force is not documented yet.

1.3 Objectives

The objective of this research is to propose unified simplified design steps for unstiffened circular bolted flange-plate connections integrating the studies done and methods proposed in the past. Following are the specific objectives of this project:

1) Conduct an extensive literature review and propose a unified design method integrating methods from the literatures. This method can be used as a design aid in the engineering industry for unstiffened circular bolted flange plate connections.
2) Carry on parametric study for different geometry using the proposed design method.
3) Compare the output results from a parametric study with other literature methods.

4) Perform FEA analysis using ANSYS for the verification of the proposed design method.
5) Perform a few design problems to illustrate the proposed method of design.

1.4 Work Plan

Literature papers related to bolted flange-plate connections are studied in detail and the papers that focused on CHS are chosen for review. The method proposed in each literature are studied in detail. A complete design step including calculation of flange-plate thickness and bolt force including prying force is compiled after selecting the part of each literature method with the same assumption of design and analysis. Different sizes and strengths of tube, bolts, and flanges are taken for the parametric study. The results are compared with the other literature methods chosen for study and integration. Few models are developed in CAD-3D and exported to ANSYS for further analysis. The results from FEA is compared with the results of the proposed method.

1.5 Thesis Outline

The remainder of this thesis is organized as follows:

Chapter 2, Literature Review, includes extensive literature review that focused on the research study and investigation of bolted flange-plate connections. It consists of the theoretical and experimental studies of the behavior of the plates under different loading conditions.

Chapter 3, Derivation of Proposed Method, comprises the detailed design steps of the methods from the literature that deals with either bending of plates or prying action or

thickness of plates. Furthermore, it includes the explanation of the analysis of proposed method and presents the design steps of the proposed method.

Chapter 4, Parametric Study of Proposed Design Method, presents the study of results using variable components in the proposed design method. It includes the influence changing the number of bolts, plate end distance, loads and material properties on the required flange-plate thickness, the prying force and the bolts force.

Chapter 5, FEA Model, a finite element model using ANSYS software is developed to compare and validate theoretical results from the proposed analytical methods of Chapter 3.

Chapter 6, Discussion of Results, analyze the results from the different analytical methods and compare them to results from the proposed method. Also, a discussion of the results from FEA is provided in this chapter.

Chapter 7, Summary and Recommendations, presents a summary of the research study, and provide recommendations for future work.

CHAPTER 2

LITERATURE REVIEW

2.1 Introduction

The foundation of this research is based on the methods adapted from an extensive literature review. The focus of this study is to generate unified design steps based on the literature for flange-plate connection. The design of circular bolted flange-plate connections mainly includes the design of flange plate and bolts due to bending moment, while considering the prying force. Hence, literature based on experimental, theoretical and numerical analysis are studied in detail.

2.2 Literature Review

2.2.1 Y.Q. Wang et al. (2013)

The main objective of this research was to analyze the behavior of flange-plate connections with eight bolts under pure-bending. Unstiffened and stiffened flange-plate connections splicing RHS and CHS were tested under four-point loading condition and related FEA were done and the results of the experiment and the FEA for all four cases were compared. In the experiment, a two-point bending test was applied on the beams using two 60 t loading capacity jacks. The connection was placed in the middle of the beam and was subjected to pure bending. The results from FEA were in good agreement with the results of the test.

From the experimental tests, the failure of unstiffened connections for RHS and CHS was due to fracture of full penetration welds between the tube and the end plates. For stiffened connections for RHS and CHS, the failure was seen due to the deformation of plates between the bolts. Hence, the design of unstiffened connections needs more care and higher safety margin as compared to the stiffened connections.

Apart from the experimental and numerical model, Y.Q. Wang proposed a theoretical design model, whose procedure combined two design models based on yield line theory and the T-stub analogy, separately. In the theoretical model, yield line theory was applied for the determination of the bending capacity of the end plates and T-stub analogy was used for the determination of the prying force. The design model includes the following steps:

1) Determination of the maximum tensile force of bolts, N_{max} , under bending moment load, M, $N_{max} = \frac{\pi * M}{n * D_{bc}}$
2) Calculation of the needed thickness of end plates, $T = \frac{f t^2 \gamma}{6}$, T is the tensile capacity of tube
3) Derive prying force, Q

This design steps were proposed for the design of flange-plate connections with eight number of bolts.

2.2.2 TIA-222-G-3 (2014)

The Telecommunications Industry Association (TIA) published a Structural Standards for Steel Antenna Towers and Antenna Supporting Structures- Addendum 3. The main objective of this publication was to provide a method of design and analysis for

the unstiffened rigid base plate. The application of this addendum was for unstiffened base plates with minimum eight number of bolts. This method was based on the yield line theory assuming both transverse and radial yield lines. It focuses on the use of ductile steel that can yield and distribute stresses to form yield lines under limit state strength loading conditions. In this method, anchor rod forces were determined based on the plastic method of analysis when the anchor rods were fully developed into the foundation. The maximum anchor rod force due to pole resultant overturning moment reaction and pole vertical reaction due to factored loads can be calculated using following equation:

$$N_{max} = [\frac{n_c * \pi * M}{n * D_{BC}} + \frac{N}{n}]$$

where, n_c = anchor rod force correction factor and the values were given in Table 1.

Table 1. Anchor Rod Correction, n_c

Number of Anchor Rods	Anchor Rod Fully Developed into Foundation	Anchor Rods Not Fully Developed into Foundation
8 – 9	1.05	1.27
10 – 11	1.04	1.27
12 – 16	1.02	1.27
> 16	1.00	1.27

After calculation pole vertical reaction, the equation for determining minimum base plate thickness was proposed for base plate bending.

$$t_{TP} > \sqrt{\frac{4 * N_{max} * x}{\emptyset_b * F_{yf} * B_{eff}}}$$

Where x was the effective moment arm of anchor rod force and B_{eff} is the total effective base plate width resisting bending, which includes bending from radial and transverse bend lines. The addendum provided a calculation of base plate thickness for base plate bending and shear. This addendum mainly focused on the design of base plate, but the provision could be extended to the circular bolted flanged plate tubular structures.

2.2.3 F. Huang et al. (2017)

The focus of this study was the mechanism of prying action in the flexible flange connection. The prying force can be observed when the flange bears tensile load or moment. In this paper, a theoretical model of the mechanism of prying action was given. In the theoretical analysis, T-shape connection was considered as its cross-section was similar to the circular flexible flange connection. There were three modes of failure as shown in Figure 8, (Fenghua Huang, Dachang Zhang, Wan Hong, Buhuli Li, 2017). Furthermore, in this case, mode 2 was considered where it was assumed that the deformation of the flange plate was equal to that of bolts. In this failure mode, the plastic hinge was formed at the weld root of the flange-plate and the bolts were pulled to failure.

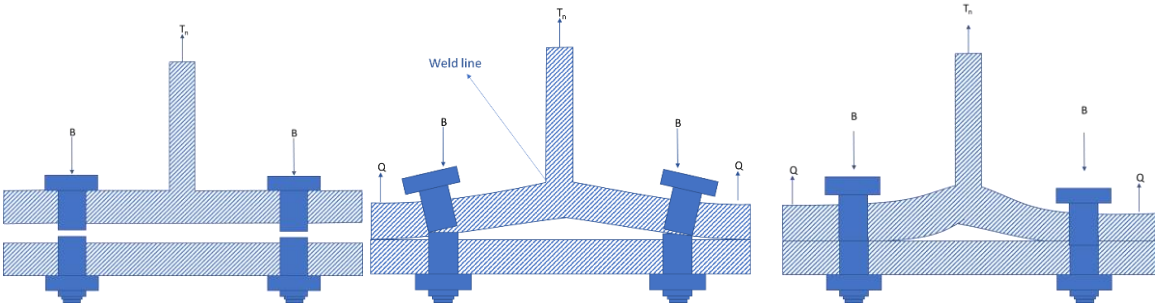

a) Mode 1 b) Mode 2 c) Mode 3

Figure 8. The three modes of failure of T-shape connection

In the theoretical analysis, factors of moment ratio α and moment arm x as shown in Figure 9 was assumed.

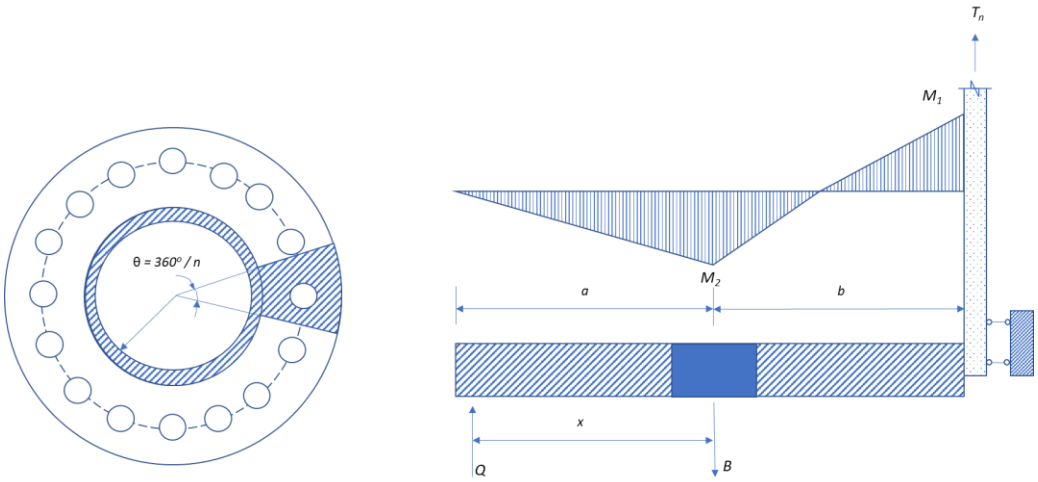

Figure 9. Prying force calculation

The equations to calculate the prying force, the bolt force and the flange plate thickness was given as follows:

$$Q = \frac{\alpha}{1+\alpha} * N_{max} * \frac{b}{x}$$

$$B = N_{max} + Q$$

$$t = \sqrt{\frac{4*N_{max}*b}{f_y*(1+\alpha)*l}}$$

Where $l = \pi * d/n$

In this research, three specimens with different thickness were tested to study the mechanical characteristics of flange plate under axial tension. The prying force cannot be measured directly, but it can be measured by comparing the bolt force with the applied load. Hence, to measure the bolt force, two strain gauges were struck symmetrical on two sides of bolts. From the results of the test, it was concluded that the prying action exists in the unstiffened flange connections and the prying force decreases with the increase of flange-plate thickness. The experimental results were compared with the finite element modeling done in ANSYS software and the results from ANSYS were in good agreement with the test results. The results from the test and FEA was to study the influence of plate thickness, the ratio of edge distance to distance between bolt center and tube and loads on bolts on the prying action. When the ratio of edge distance and distance from the bolt center to the tube was high, prying action was low, however, when the ratio was greater than 1, it will not have much influence on the prying action. Greater the bolt preload, more prying action can be observed. After the test and FEA, F. Huang (2017) proposed the modified formula for the theoretical calculation of the prying force.

$$Q = \frac{1}{2} * N_{max} * \frac{1}{0.6\eta}$$

where, η is the ratio of edge distance to the distance from the bolt center to the tube. The modified formula of prying force fit well with the FEA result and it considered hogging moment at the weld line of the flange plate and location of prying resultant.

2.2.4 H.Z. Deng (2009)

This study investigated three specimens under monotonic loading to verify the reliability of flange joint and study the rotational axis location of bolts. The steel transmission poles were subjected to bending moment (M) and axial force (N) and during the test, the specimens were set such that force was applied eccentrically by the hydraulic jack placed at a certain distance from the poles. The tubes and the flange plates were welded using full penetration weld. Two of the specimens had annular rings inside the tube (stiffening ribs). From the test result, it was concluded that the annular plate inside the tube reduced stress concentration in the tube and provides additional stiffeners to the flange plates. Additionally, no prying force was present on the tension side of the plates. In the conventional design, bolts were subjected to axial tensile force and the critical section was at the surface of the tube. From the experimental and FEA results, the new critical section at a distance of 0.8r from the tube center was proposed for the calculation of the bolt force. The bolt force calculated using this new proposed critical section was 17.3% higher than the conventional design.

2.2.5 G M Pinfold (1994)

This paper investigated the types of lack-of-fit of bolted flange plate connections. Basically, there were two types of lack-of-fit that may occur either separately or together. The first type was the one where the flange was not truly normal to the tube which may be due to welding distortion and this type of fit can be recovered by adding gusset plates. The second type was the one where, the flange was normal to the tube, but two flanges were separated at the circumference. This type may be the result of mismatching of the pair of flange plate by the manufacturers and it can be reduced by using bolts correctly.

To prevent the failure of the tubular structures due to this kind of lack-of-fit, the flange plate faces should be arranged correctly with proper installation of bolts.

The literature review provided a thorough understanding of the method of analysis of circular bolted flange plate connections. Besides, it provided different cases of failure of the tubular structure, discussed of prying action on unstiffened connections and provided different approaches to calculate flange plate thickness.

CHAPTER 3

DERIVATION OF PROPOSED DESIGN METHOD

3.1 General

The objective of this study is to propose simplified design steps for circular bolted flange plate connections by adapting the basic assumptions and concept of current design methods. The study will provide unified design steps integrating the theoretical models proposed in the literature. Basically, this study was focused on the steel CHS transmission and distribution poles with unstiffened circular bolted flange-plate connections.

3.2 Current Design Methods

3.2.1 Method 1: Y.Q. Wang et al. (2013)

This model puts forward a design model based on yield line theory and T-stub analogy to calculate flange plate thickness, prying force and bolt force. The design procedure was based on the two models, bending capacity determined for yielding of the end plate and bending capacity determined for high-strength bolts. The basic assumptions made for the analysis were stated as follows:

- The flange-plate connection should be stronger than the HSS member that it splices.

- The failure of end plates can be seen before bolt failure and bending capacity of connection was controlled by the end plates.
- Full penetration weld was used between the tube and the end plates and the effect of the weld was neglected in the design.
- For unstiffened connections, more safety margin should be considered.

In this theoretical model, since it was assumed that the connection is stronger than the tube, the flange-plate thickness was derived from the bending capacity of the tube. For unstiffened connection, to meet the safety demand, actual yield capacity is assumed to be 1.5 times the design value. Considering all these points, and based on two design models, Y.Q. Wang (2013) proposed the following design steps:

a) Derive the maximum tensile force of bolts under bending moment, M.

$$N_{max} = \frac{\pi * M}{n * D_{bc}} < N_t^b$$

b) Derive the needed end plate thickness, t_1

$$T = \frac{f * t_1^2 * \gamma}{6}; \quad \gamma = 8 * \left(\frac{r+b}{b}\right) * \tan\left(\frac{\pi}{2n}\right)$$

c) Calculate t_c and t_d;

The maximum end plate thickness without considering prying action is,

$$t_c = \sqrt{\frac{4 * N_t^b * b}{B_{eff} * f}}$$

The end plate thickness while considering prying action and when the end plate is in double curvature is, $t_d = \sqrt{\frac{2 * N_t^b * b}{B_{eff} * f}}$

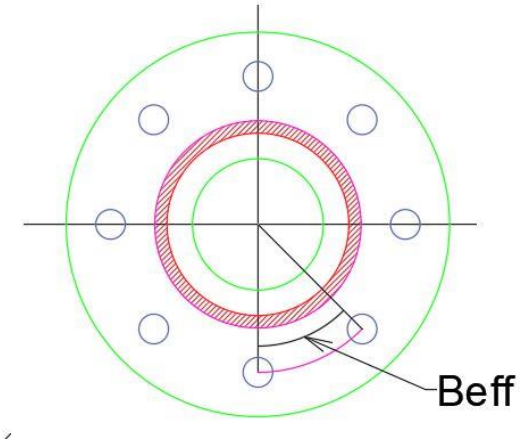

Figure 10. Calculation of effective width

where, B_{eff} is the average length between two yield lines for a single yield region.

d) Check if $t_1 < t_c$ and choose t2 as maximum value between t1 and td.

e) Derive prying force,

$$Q = \frac{\alpha}{1+\alpha} * \frac{b}{a} * N_{max} \quad ; \alpha = 1$$

f) Calculate bolt force, $B = N_{max} + Q < N_t^b$

g) If step (f) is true, take t2 as the design value of flange plate thickness.

There were few limitations to this design model and they are stated as follows:

- This method mainly focused on the calculation of maximum tensile force of bolts under bending moment only. There was no consideration of the axial tensile force that should be transferred to the bolts.
- This model was limited to the use of eight number of bolts only. Since the behavior of the connection varied with the change in the arrangement of bolts, this

model may not be applicable to the connections with the number of bolts other than eight.

3.2.2 Method 2: TIA-222-G-3 (2014)

This method was for the tubular pole unstiffened base plate. The study was performed on the unstiffened base plates with round center openings with galvanizing drainage, tubular steel poles with round or 6 or more sided cross-sections, base plates supported on levelling buts with or without grouting, and a minimum of 8 anchor rods equally spaced. The basic assumptions of this design method were:

- Base plate bending strength was determined based on the yield line theory assuming both transverse and radial yield lines as shown in Figure 11.
- Ductile steel was used which can yield and distribute stresses to form yield lines under limit state strength loading conditions.
- Anchor rod forces were determined based on the plastic method of analysis when the anchor rods were fully developed into the foundation.

Based on these assumptions, theoretical design procedure of the base plate were:

a) Derive maximum anchor rod force due to factored pole loads,

$$N_{max} = \frac{n_c * \pi * M}{n * D_{bc}} + \frac{N}{n}$$

where, n_c is the anchor rod force correction factor from Table 1., Mu is the pole resultant overturning moment reaction due to factored loads on anchor rod group and Ru is the pole vertical reaction due to factored loads on anchor rod group.

b) Derive the minimum base plate thickness required for bending using the following equation:

$$t_P \geq \sqrt{\frac{4 * N_{max} * b}{0.9 * f_{yf} * B_{eff}}}$$

where, b is the effective moment arm of anchor rod force or distance between the tube and the bolt circle and Beff is the total effective base plate width resisting bending.

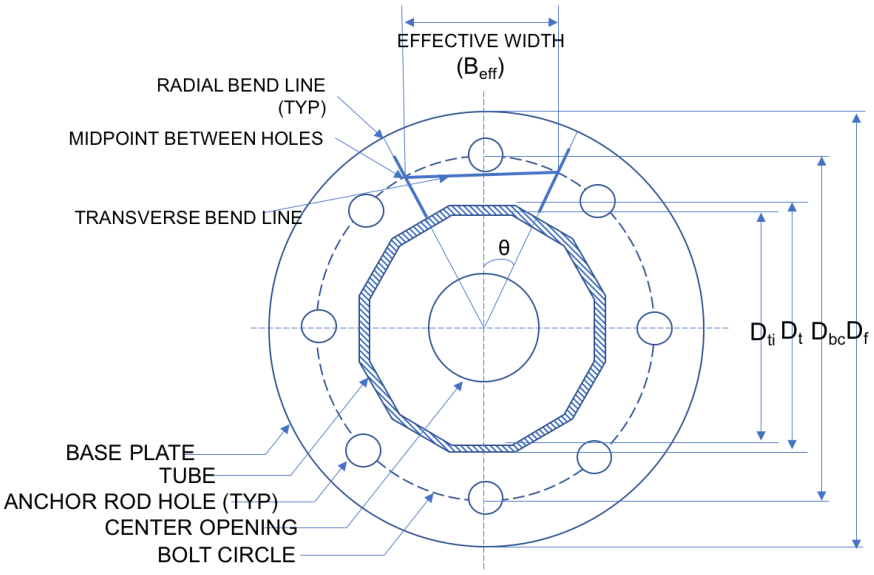

Figure 11. Symbolic representation for TIA method

$$b = 0.5 * (D_{bc} - D_T)$$

$$B_{eff} = B_{et} + B_{er}$$

$$B_{et} = D_{bc} * sin\theta$$

$$B_{er} = (D_P - D_T) * sin\theta$$

$$\theta = minimum\ of\ \theta_1, \theta_2\ and\ \theta_3$$

$$\theta_1 = \frac{\pi}{n}\ radians$$

$$\theta_2 = sin^{-1}\left[\frac{12*t_P}{D_{bc}}\right] radians, where\ 12(t_P) \geq D_{bc}, \theta_2 = \theta_1$$

$$\theta_3 = cos^{-1}\left[\frac{D_{bc}+D_T}{2*D_{bc}}\right] radians$$

Where, D_T = Diameter of external tube

D_P = Diameter of base plate

The limitations of this design method were:

- This method was designed for the base plates where, bolts were developed into the foundation.
- The use of n_c might not be applicable in the case of flange-plate connections.
- The design did not consider the existence of prying action.

3.2.3 Method 3: F. Huang et al. (2017)

This method is focused on the mechanism and calculation theory of prying force flexible flange-plate connections. The prying action is more in the unstiffened flange-plate connection. The loading conditions for the flexible flange include a tensile force in the splice that causes the flange plate to deform. In the tensile bolted connections, the prying force occurs at the edge of the plate. Total force on bolt is the sum of prying force and the forces due to applied loads. In this method, a failure mode is assumed in which a plastic hinge is formed in the flange plate at the weld line and the bolts were pulled up to failure, (Fenghua Huang, Dachang Zhang, Wan Hong, Buhuli Li, 2017).

As shown in Figure 12, cross-section of one section is shown in the figure (b). Applying equilibrium conditions as in Figure 12, the basic equation for the calculation of prying force is as follows:

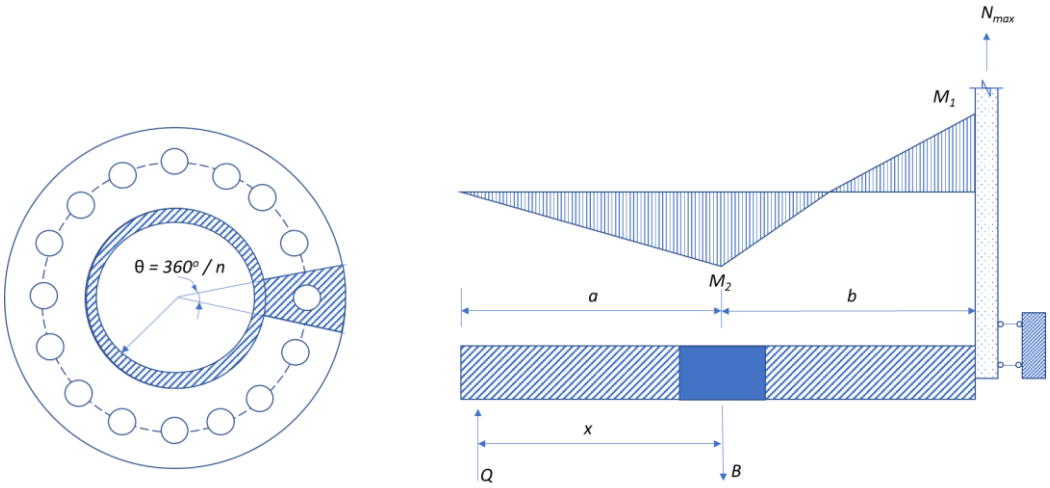

a) Top view b) Cross-section of one section

Figure 12. Calculation model of prying action

$$M_1 + M_2 - N_{max} b = 0 \quad (1)$$

$$M_2 = Q.x \quad (2)$$

Where,

M1 = the hogging moment at the root of flange plate

M2 = the sagging moment at the bolt line

Nmax = the maximum forces due to applied loads

Q = Prying force

x = the arm of the prying force

moment ratio, $\alpha = \frac{M_2}{M_1}$

equation (1) and (2) can be written as,

$$\alpha M_1 = Q.x$$

$$M_1 + \alpha M_1 - T_n.b = 0$$

Which gives,

$$Q = \frac{\alpha}{1+\alpha}.T_n.\frac{b}{x}$$

Based on the FEA analysis and theoretical analysis, considering that the flange-plate bends in the parabolic shape, and no failure of bolts, it was proposed that:

$\alpha = 1\ and\ x = 0.6b$

Modified formula for prying force:

$$Q = \frac{1}{2}.T_n.\frac{1}{0.6}$$

3.3 Proposed Design Methodology

The design method of determining the flange plate thickness along with the calculation of prying force and total bolt force for unstiffened circular bolted flange plate connection was done in this study. This study involved the connections with minimum eight number of bolts. The proposed design method was based on the yield line method of analysis considering equilibrium, yield mechanism and limit state strength loading conditions. Full penetration welds were applied to the tube and the flange-plate. The effect of welds between circular tube structure and flange plate were not considered. It is assumed that the flange plate failure occurs before bolt failure. Plastic hinge is formed both at the weld line and bolt line, and deformation of flange plate is larger than those of bolts. This is the third mode of failure of the T-shape connections and shown in Figure 13. In the analysis, neutral axis is at the center line of the pole and the critical section for bending of the plate is at the perimeter of external tube and the bolt circle as shown in Figure 14. Also, in the structure, it is assumed that the distance between the flange-plate and the bolt circle, a and the distance between the bolt circle and the external tube, b were same.

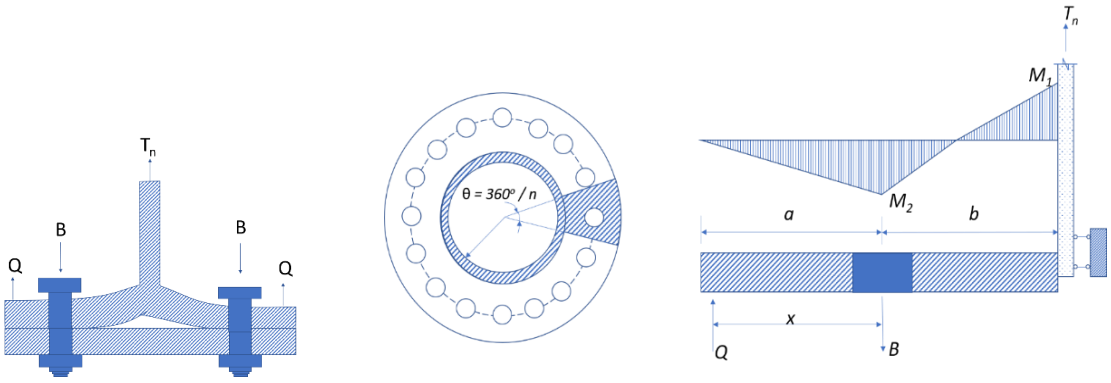

Figure 13. Prying force calculation

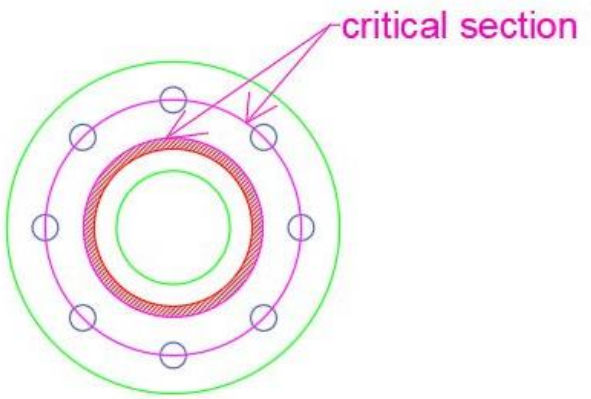

Figure 14. Critical sections

The design steps showing the theoretical procedure of the proposed method is as follows:

a) Calculate the maximum tensile force of bolts, N_{max}:

The applied force and moment were shown in Figure 15.

$$N_{max} = \frac{\pi * M}{n * D_{bc}} + (\frac{N}{n}) \leq N_t^b$$

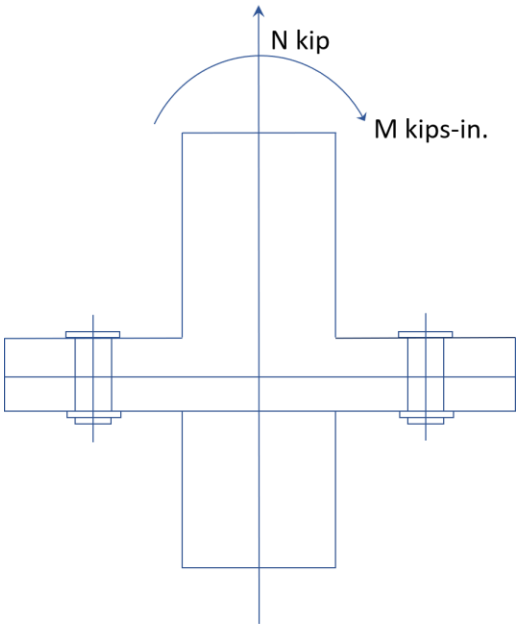

Figure 15. Application of forces

N_t^b = Design value of bolt tensile capacity

M = Bending moment which the connection should transfer

N = Tensile force which a bolt should transfer

n = number of bolts

D_{bc} = Diameter of bolt circle

b) Calculate Prying Force, Q:

$$Q = \left(\frac{1}{2}\right) * N_{max} * \left(\frac{1}{0.6}\right) = 0.833N_{max}$$

This equation showed that the prying force is based on the maximum tensile force on bolt. This ultimately showed that the prying force calculated here depends on the bending moment and the axial tensile load.

c) Derive Bolt Force, B:

Total force on one bolt are shown in Figure 16 and the equation for its calculation is, $B = N_{max} + Q \leq N_t^b$

This equation serves as a check for the design. If this condition is not true, then the input geometry could be altered or number of bolts could be changed and then calculations should be again started and checked.

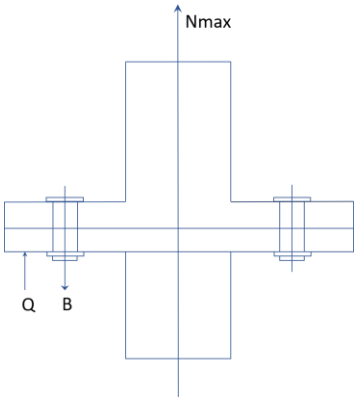

Figure 16. Total force on bolts

d) Calculate thickness of flange plate, t_f:

$$t_f \geq \sqrt{\frac{4 * N_{max} * b}{f_{yf} * B_{eff}}}$$

b = distance between flange-plate and bolt circle

f_{yf} = flange-plate design yield strength

B_{eff} = total effective base plate width resisting bending

$B_{eff} = \frac{\pi(D_{bc}+D_t)}{2*n}$

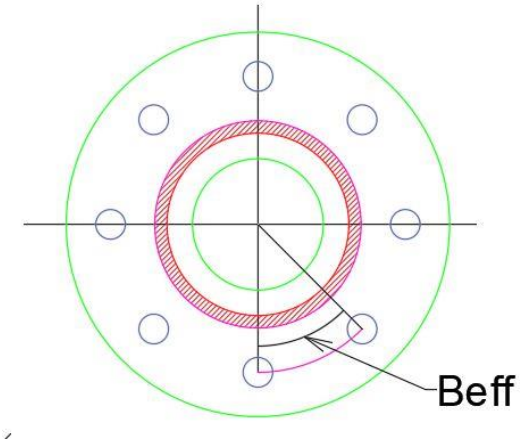

Figure 17. Effective width

In the calculation of flange-plate thickness, N_{max} was used instead of B. The condition for the design to be safe was given in the third step, in the calculation of bolt force. If this condition was true, then the design of flange-plate using maximum tensile loads due to applied loads would be safe.

A flow chart showing a complete design procedure of the proposed method is given in Figure 18 .

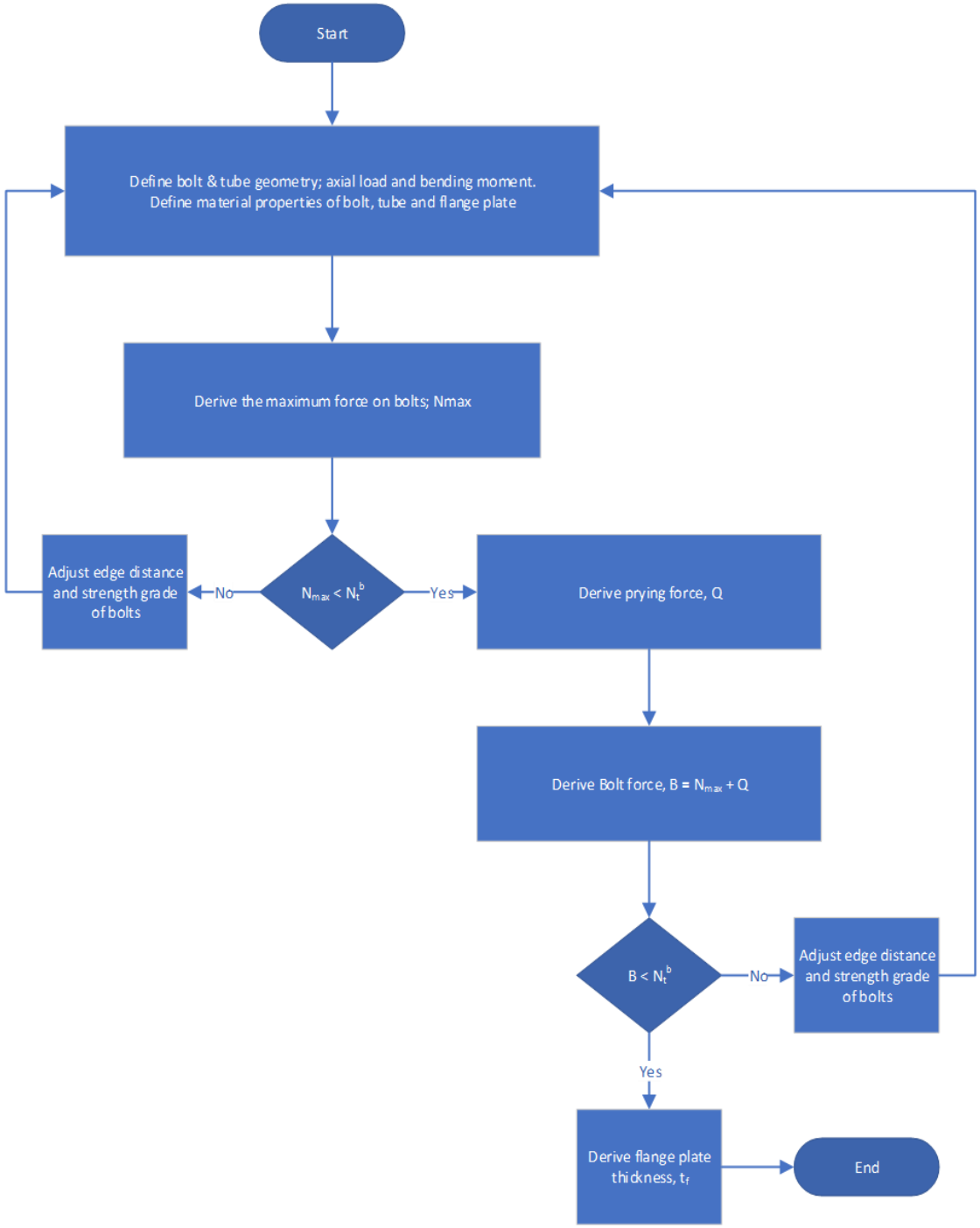

Figure 18. Flow chart showing design procedure of proposed method

3.4 Summary

The design steps in the proposed method addressed the limitations mentioned in the current design methods. In method 1, only bending moment M was considered for determining the maximum tensile force of bolts (Y.Q. Wang et al., 2013) and in the design of base plate, the calculation of the vertical force due to factored loads on anchor rod group included bolt correction factor, "n_c" (TIA, 2014) was considered. Considering these two methods, for the calculation of the maximum tensile force of bolts, the proposed method considered both the axial tensile force and the bending moment. Since prying action can be seen more in the unstiffened connection than in the stiffened connection, the determination of prying force while calculating bolt force should be included in the design. The formula for the calculation of prying force in the proposed method is the formula suggested after experimental and numerical verification by F. Huang, 2017. In the addendum 3 proposed by TIA, 2014, there is no mention of the existence of the prying action. The theoretical derivation of flange plate thickness under pure bending for bolted flange-plate connection with eight number of bolts was proposed in the Journal of Construction Steel Research 84 (Y.Q. Wang,2013) and the base plate thickness formula considering radial and transverse yield lines was given in TIA, 2014. From statics and considering bolt circle and external tube perimeter as two yield lines, and for eight or greater number of bolts, the flange-plate thickness was proposed in this design method.

Table 2. Summary of methods

S.N	Methods	Assumptions	Results	Limitations
1.	Y.Q Wang et al. (2013)	- Flange-plate was stronger than the material it splices. -Failure of bolts occured after failure of flange-plate. - Effect of weld was neglected	- $N_{max} = \frac{\pi * M}{n * D_{bc}}$ - $Q = \frac{\alpha}{1+\alpha} * \frac{b}{a} * N_{max}$ -$B = N_{max} + Q < N_t^b$ -$t_f = \frac{f * t^2 * \gamma}{6}$	- Consideration of moment only while calculating N_{max}. - Limited to the use of 8 number of bolts only.
2.	TIA-222-G-3 (2014)	- Base plate strength determined based on yield line theory assuming both transverse and yield lines. - Ductile steel was used which can yield and distribute stresses. - Anchor rod forces were determined based on the plastic method of analysis.	- $N_{max} = \frac{n_c * \pi * M}{n * D_{bc}} + \frac{N}{n}$ -$t_f \geq \sqrt{\frac{4 * N_{max} * x}{0.9 * f_{yf} * B_{eff}}}$	- This method is designed for the base plates where, bolts were developed into the foundation. - The use of n_c may not be applicable in the case of flange-plate connections. -The design does not consider the existence of prying action.
3.	F. Huang et al. (2017)	- A failure mode where a plastic hinge is formed in the flange plate at the weld line and the bolts were pulled to failure	- $Q = \frac{1}{2} . N_{max} . \frac{1}{0.6}$	- This method describes about prying action only.

4.	Proposed Method	- This method was based on the yield line method of analysis considering equilibrium, yield mechanism, and limit state strength loading conditions. - Effect of weld was not considered. Deformation of flange-plate was larger than bolts.	-$N_{max} = \frac{\pi * M}{n * D_{bc}} + (\frac{N}{n}) \leq N_t^b$ -$Q = \left(\frac{1}{2}\right) * N_{max} * \left(\frac{1}{0.6}\right) = 0.833 N_{max}$ -$B = N_{max} + Q \leq N_t^b$ -$t_f \geq \sqrt{\frac{4 * N_{max} * b}{f_{yf} * B_{eff}}}$	- Experimental verification of this method is yet to be done. -The design steps were for the unstiffened circular bolted flange-plate only.

CHAPTER 4

PARAMETRIC STUDY USING PROPOSED DESIGN METHOD

4.1 General

The design steps for the proposed design method is used step-wise as shown in Figure 18. This chapter deals with the use of those design steps and influence of variable geometry, applied loads, and plate material on the flange-plate thickness and the prying force.

4.2 The influence of bolt arrangement

For the study of the influence of bolt arrangement on the flange thickness and prying action, three design examples were considered and in each design example, three cases were taken with a variable number of bolts as shown in Table 3. and the results are shown in Figure 19. In this study, minimum 8 number of bolts are used, so variable number of bolts used are 12, 16 and 20. Also in the study it was assumed that the distance a and distance b are same. Comparing the results of three design examples with a different number of bolts or different bolt arrangement, it was found that the bolt arrangement has no influence on the flange-plate thickness as it depends on the maximum tensile force of bolts, the distance between tube and bolt circle and flange-plate material properties. However, it is clear from Figure 19, that prying force is greater when the

distance between bolts is greater. When bolts were arranged closer to each other, the prying action is reduced.

Table 3. Design examples with variable number of bolts

	Predefined Parameters								Step-wise calculation						
I D	Tube dia, Dt (in.)	b (in.)	No. of bolts, n	Flange dia, Df	fyf (ksi)	N kips	M Kips-in	N^t_b Kips	Dia of bolt circle	B_{eff} (in.)	N_{max} (kips)	Q (Kips)	B (kips)	Check	tf (in)
Design Example 1															
A1-1	6.61	1.41	12	12.2	60	28	664	45	9.44	2.10	20.7	17.2	37.9	OK	1.01
A1-2	6.614	1.417	16	12.282	60	28	664	45	9.448	1.576	15.542	12.947	28.489	OK	1.017
A1-3	6.614	1.417	20	12.28	60	28	664	45	9.448	1.261	12.43	10.35	22.79	OK	1.017
Design Example 2															
A2-1	8.622	1.299	12	13.81	60	35	885	45	11.22	2.596	23.55	19.62	43.18	OK	0.934
A2-2	8.622	1.299	16	13.81	60	35	885	45	11.22	1.947	17.66	14.71	32.38	OK	0.934
A2-3	8.622	1.299	20	13.818	60	35	885	45	11.22	1.558	14.134	11.773	25.91	OK	0.934
Design Example 3															
A3-1	27.559	1.968	12	35.431	60	150	1200	45	31.495	7.726	22.47	18.717	41.19	OK	0.651
A3-2	27.559	1.968	16	35.431	60	150	1200	45	31.495	5.795	16.852	14.038	30.89	OK	0.651
A3-3	27.559	1.968	20	35.431	60	150	1200	45	31.495	4.636	13.482	11.23	24.71	OK	0.651

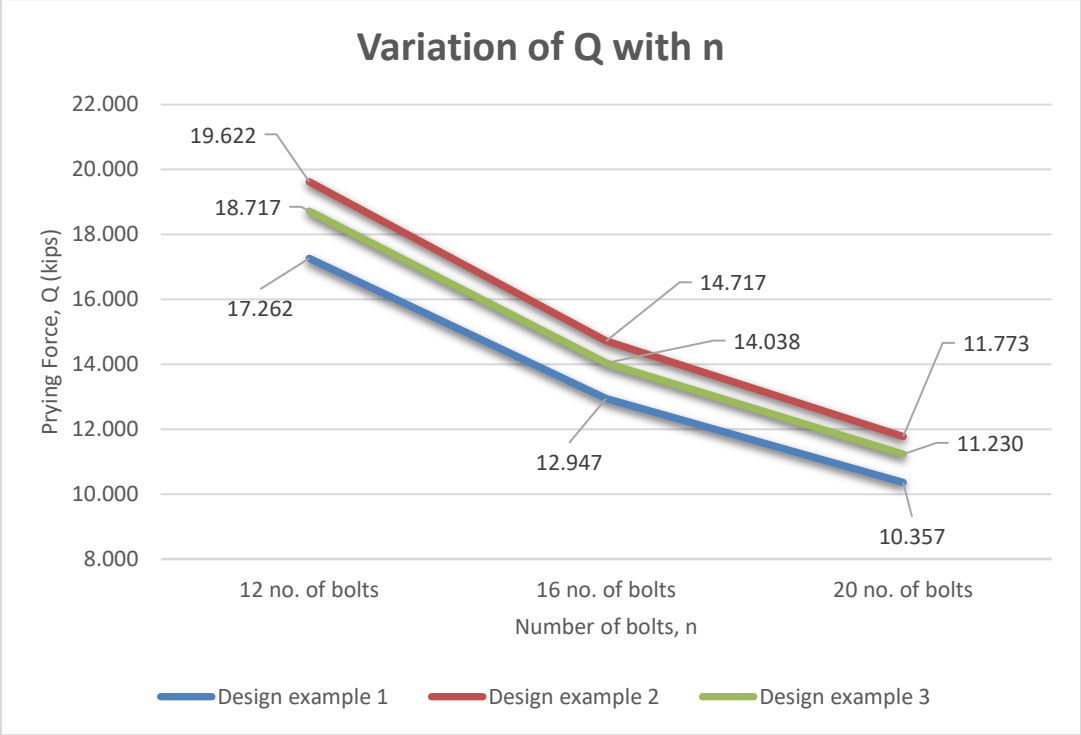

Figure 19. The curve showing variation of prying force with number of bolts

4.3 The influence of distance a and b

The distance between tube and bolt circle, b and the bolt circle and flange plate, b were assumed to be same in this research. Calculation of the prying force, the bolt force, and the flange-plate thickness are shown in Table 4 for three cases with variable a and b for three design examples. The results comparing the results of these three design examples with every three cases are shown in Figure 20 and Figure 21. For the same tube diameter and number of bolts, changing the value of a and b will change the size of the flange-plate. Since the calculation equations considered b in the design, variable value of b is shown in Table 4. However, the value a and b are the same. It is clear from Figure 20

that for the higher value of b, thicker flange-plate is required. For the same tube geometry, as the value of b increases, the bolt circle diameter also increases, and the maximum tensile force of bolts will decrease and accordingly, the prying force will also decrease. This kind of nature is represented in Figure 21.

Table 4. Design examples with variable distance between the tube and the bolt circle

	Predefined Parameters								Step-wise calculation						
S.N	Tube dia, Dt	b (in.)	No. of bolts, n	Flange dia, Df	fyf (ksi)	N (kips)	M (Kips-in)	$Nt_{b(}$ Kips)	Dia of bolt	B_{eff} (in.)	N_{max} (kips)	Q (Kips)	B (kips)	Check	tf (in)
Design Example 1															
B1-1	6.61	1.29	16	11.8	60	28	664	45	9.21	1.55	15.8	13.2	29.1	OK	0.99
B1-2	6.614	1.417	16	12.282	60	28	664	45	9.448	1.576	15.542	12.947	27.418	OK	1.017
B1-3	6.614	1.626	16	13.11	60	28	664	45	9.866	1.617	14.95	12.46	27.41	OK	1.056
Design Example 2															
B2-1	8.622	1.299	20	13.81	60	35	885	45	11.22	1.558	14.13	11.77	25.91	OK	0.934
B2-2	8.622	1.417	20	14.29	60	35	885	45	11.45	1.576	13.87	11.56	25.44	OK	0.961
B2-3	8.622	1.626	20	15.126	60	35	885	45	11.874	1.609	13.452	11.205	24.66	OK	1.003
Design Example 3															
B3-1	27.559	1.299	30	32.755	60	150	1200	45	30.157	3.02	9.1649	7.6343	16.8	OK	0.540
B3-2	27.559	1.417	30	33.227	60	150	1200	45	30.393	3.033	9.1325	7.6074	16.74	OK	0.562
B3-3	27.559	1.626	30	34.063	60	150	1200	45	30.811	3.055	9.0765	7.5607	16.64	OK	0.598

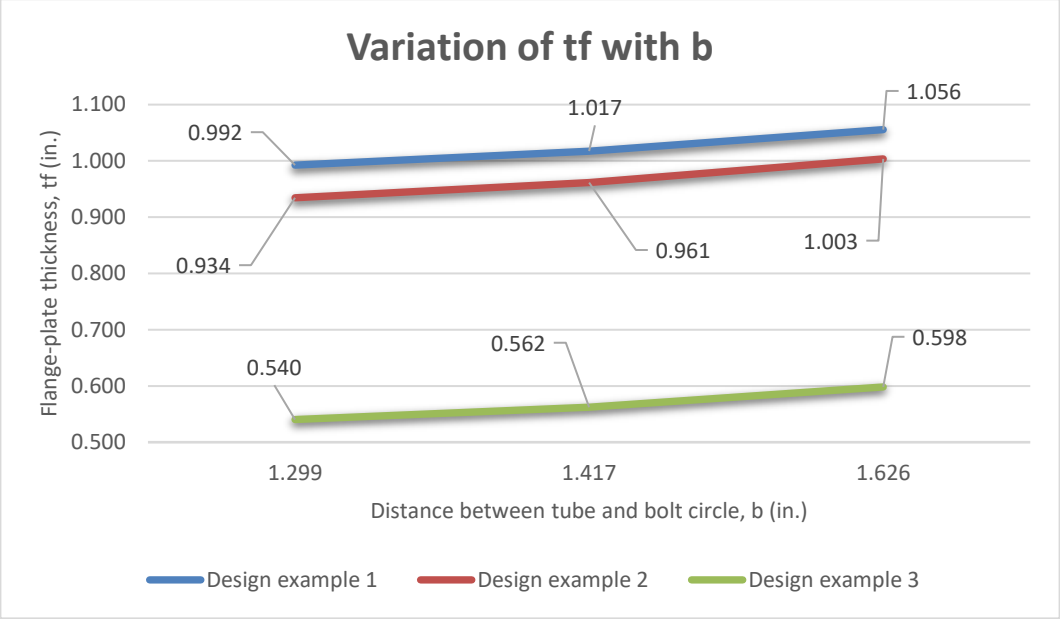

Figure 20. The curve showing variation of flange-plate thickness with end distance

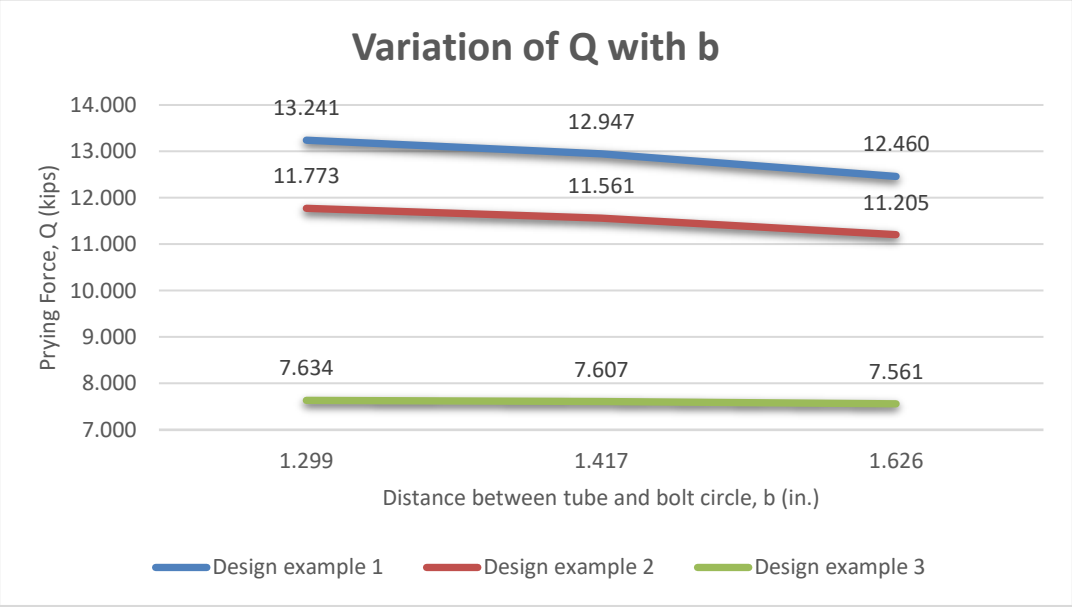

Figure 21. The curve showing variation of prying force with end distance

4.4 Summary

The parametric study clarified the influence of different parameters on the prying force and the flange-plate thickness. In the literature that was reviewed, experimental and theoretical calculations were explained. The current parametric study helped validate the proposed method. The results from the parametric study show similar pattern as in the literature paper by F. Huang. The study showed that the number of bolts and the distance a and b had the influence on the prying force.

CHAPTER 5

FEA MODEL

5.1 General

Finite Element Analysis (FEA) using ANSYS was performed to check if the flange-plate design using the proposed method is safe or not. Also, FEA is used as a tool to validate the theoretical results. First, the procedure of modeling is described in the following sections of this chapter. In ANSYS workbench, the static structure was used to input the engineering data and geometry. The modal analysis was done using Mechanical ANSYS Multiphysics. In this study, linear static analysis was used, and the analysis did not depend on time. The default engineering properties for structural steel in the analysis were given below:

Material field variable, Temperature: $71.6^{\circ}F^{-1}$

Density: 0.2836 lb in^{-3}

Coefficient of thermal expansion: $6.667*10^{-6}$ psi

Young's modulus of elasticity: $2.908*10^{7}$ psi

Poisson's ratio: 0.3

Bulk modulus: $1.6667*10^{11}$ Pa

Shear modulus: 7.6923*1010 Pa

Tensile yield strength: 60000 psi

Compressive yield strength: 60000 psi

Tensile ultimate strength: 66717 psi

5.1.1 Geometry

First, models were generated using CAD 3D and then the models were exported to ANSYS workbench. The geometry after exporting to ANSYS is shown in Figure 22.

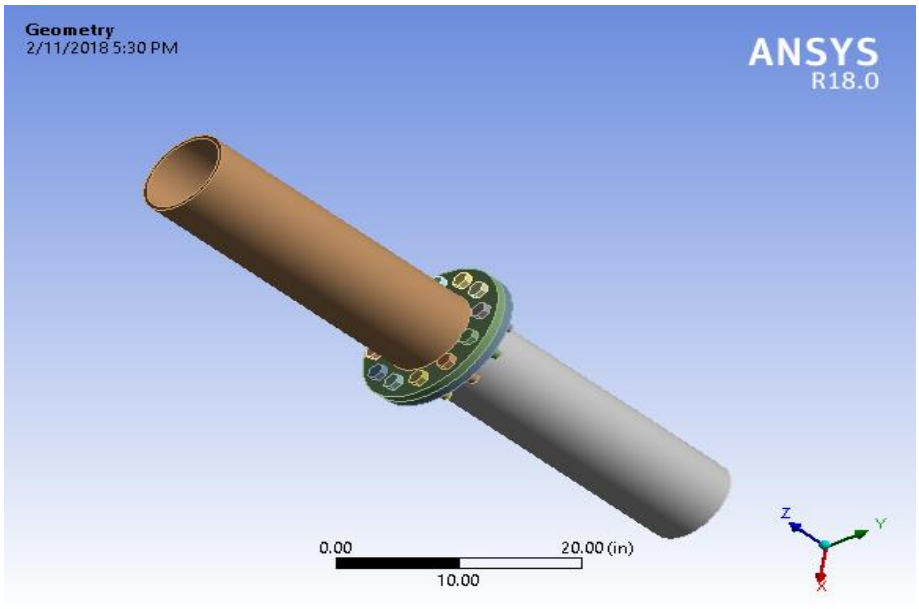

Figure 22. Design model geometry

5.1.2 Connections

The connections between two steel structures were defined based on the splices and the loads they may transfer. In two example models, the connection between the tube and the flange-plate and between nuts and bolts were assigned as the bonded connection. In the bonded connection, there is no sliding and no gap. The connection between the bolt head and the flange-plate is assigned as frictional with frictional co-efficient 0.3 and the connection between bolt and bolt hole in flange-plate is assigned as frictionless.

Furthermore, the connection between nut surface and flange-plate, and the connection between flange to flange-plate were assigned as frictional with frictional co-efficient 0.2. Instead of using 0.3, 0.2 frictional co-efficient was used, because in these two connections, sliding action was assumed to be more. In the frictional connection, the contact and target body can translate into the normal and the tangential directional. In the frictionless connection, there is a gap between two surfaces, and the body can slide but the nodes in contact are restrained against displacement in the normal direction.

5.1.3 Meshing

For the modal analysis, the structure was divided into smaller divisions and then analyzed. This process was done by generating a mesh in the structure. After defining the type of connections, program-controlled mesh could be generated. All other default data were selected except sizing. There is option for coarse, medium and fine sizing of the mesh. While choosing fine and medium size meshing, the program took much longer time to run. Therefore, coarse size meshing was chosen for the analysis. The figure with meshing is shown in Figure 23.

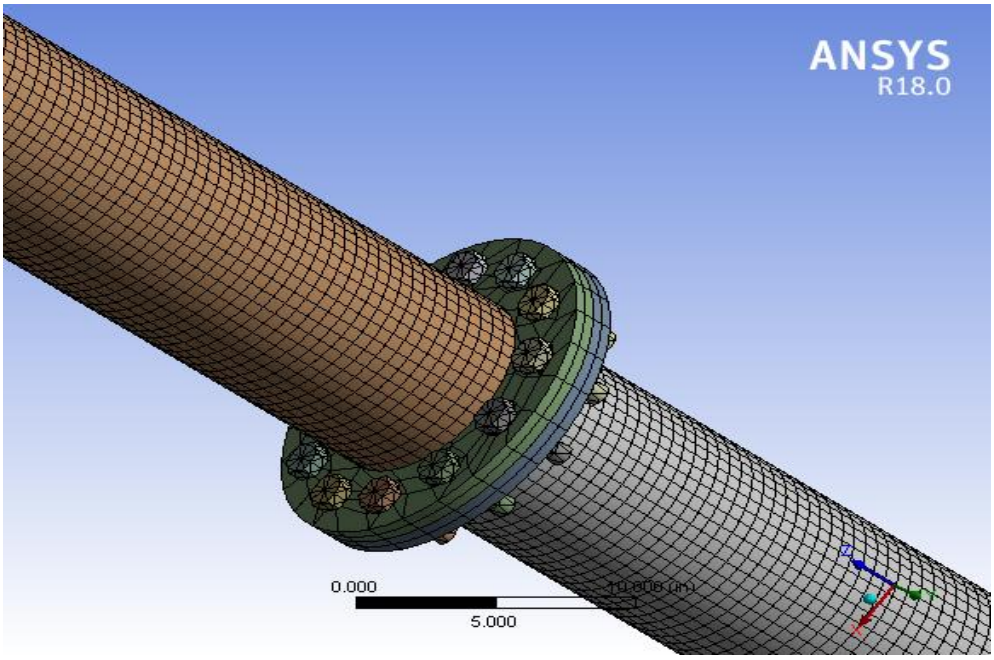

Figure 23. Design model meshing

5.1.4 Boundary conditions

For both cases, the surface of the lower tube was assigned as fixed support and force and moment were assigned at the top face of the tube. Since the parametric study using FEA was to validate the theoretical study, the failure loads were used from the loads used in the theoretical study. The loads should be such that they do not exceed the design tensile loads.

5.2 Parametric Study

For the parametric study of the proposed method, FEA was done by running models with different parameters in ANSYS. For the study of each parameter, two design example models were used. The results of this study were explained in the following sub-sections. For each study, the normal stress and equivalent strain were studied and

compared. The normal stress observed in the FEA from each case described in sections 5.2.1 and 5.2.2, were compared with the theoretical calculation and the comparative results were shown in Table 5 and Table 6. As shown in these mentioned tables, the numerical results of normal stress from FEA were close to the theoretical calculation.

Besides stress, an equivalent strain was also studied. From the FEA result, the strain was greater in the high tension zone as shown in Figure 24, Figure 25, Figure 26, and Figure 27. In all cases, strain was higher in the tension zone between the bolt circle and the face of the tube.

5.2.1 Variable number of bolts

Two design models were run in ANSYS following all the steps mentioned in the 4.2 section of this chapter. The parameters of the design models were the first two examples (A1-1 and A1-2) from Table 3. After applying the axial load and bending moment in the model, it was run to get results. The comparative study of normal stress at the bolts from FEA and theoretical calculation is shown in Table 5 and the equivalent strain of two models are given in Figure 24 and Figure 25.

The theoretical calculation for normal stress at the bolts are:

$\sigma = \frac{N_{max}}{A}$, σ = normal stress, N_{max} = maximum tensile force on bolts, A = area of bolts

For A1-1, N_{max} = 20720 lbs, A = 0.70138 in^2

$$\sigma = \frac{20720}{0.70138} = 29541\ psi$$

For A1-2, N_{max} = 15542 lbs, A = 0.70138 in^2

$$\sigma = \frac{15542}{0.70138} = 22159\ psi$$

Table 5. Comparison of normal stress between the theoretical calculation and FEA for Model A1.

Examples	Theoretical calculation (psi)	FEA (psi)	Theoretical/FEA
A1-1	29541	30740	0.96
A1-2	22159	23589	0.94

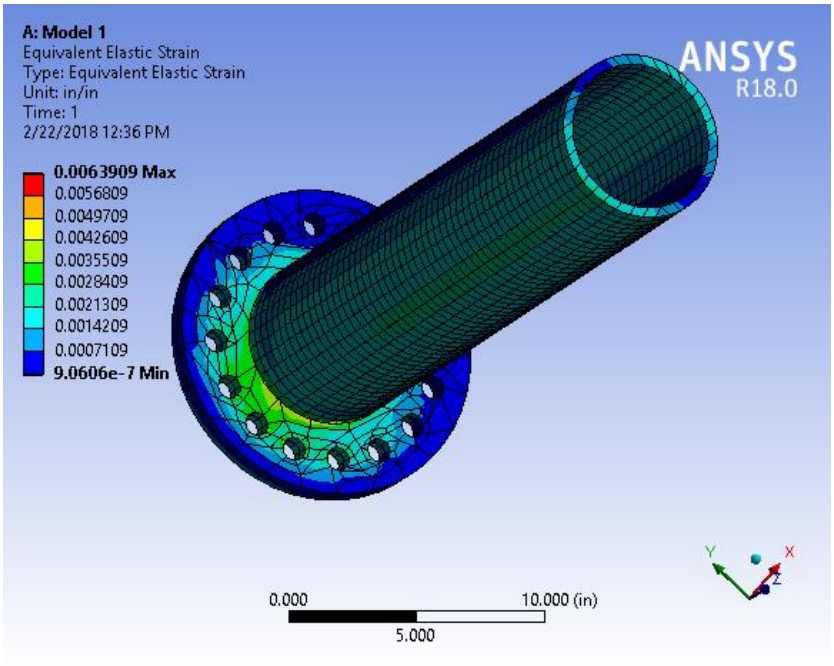

Figure 24. FEA result - Equivalent strain of A1-1

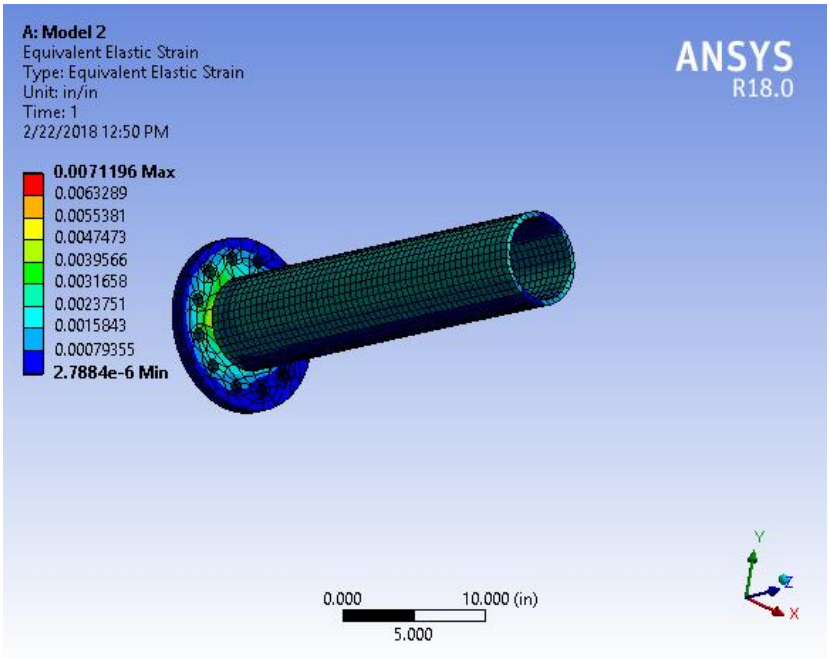

Figure 25. FEA result - Equivalent strain of A1-2

5.2.2 Variable end distance between tube and bolt circle

Two design models were run in ANSYS following all the steps mentioned in the 4.3 section of this chapter. The parameters of the design models were the first two examples (B1-1 and B1-2) from Table 4. After applying the axial load and bending moment in the model, it was run to get results. The comparative study of normal stress at the bolts from FEA and theoretical calculation is shown in Table 6 and the equivalent strain of two models were given in Figure 26 and Figure 27.

The theoretical calculation for normal stress at the bolts are:

$\sigma = \frac{N_{max}}{A}$, σ = normal stress, N_{max} = maximum tensile force on bolts, A = area of bolts

For B1-1, N_{max} = 15890 lbs, A = 0.70138 in^2

$$\sigma = \frac{15890}{0.70138} = 22655\ psi$$

For B1-2, N_{max} = 15542 lbs, A = 0.70138 in^2

$$\sigma = \frac{15542}{0.70138} = 22159\ psi$$

Table 6. Comparison of normal stress between the theoretical calculation and FEA for Model B1.

Examples	Theoretical calculation (psi)	FEA (psi)	Theoretical/FEA
B1-1	22655	25172	0.9
B1-2	22159	23789	0.93

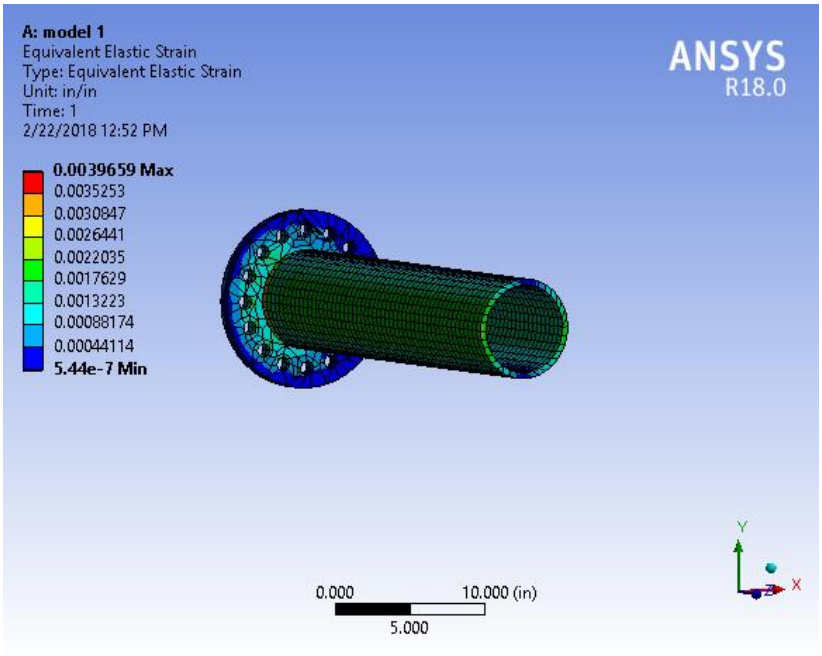

Figure 26. FEA result - Equivalent strain of B1-1

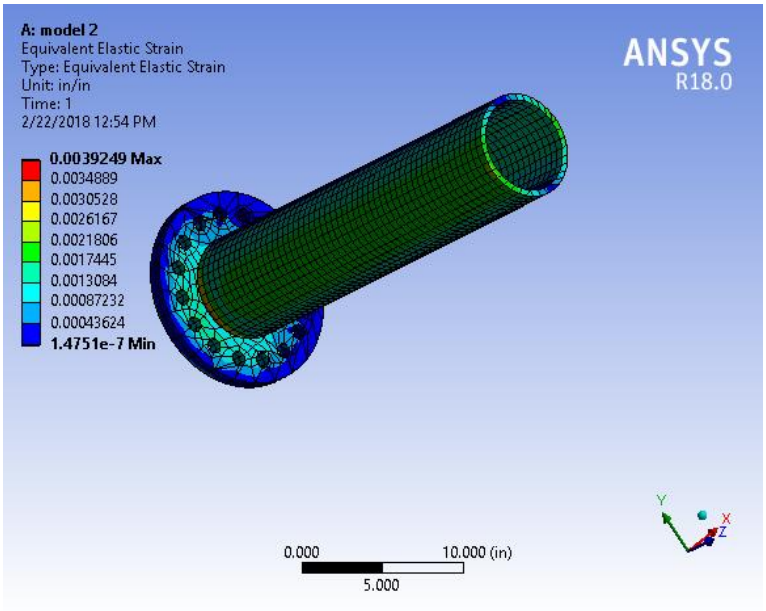

Figure 27. FEA result - Equivalent strain of B1-2

5.3 Summary

The results explained in this chapter were in good agreement with the theoretically calculated results. The nature of distribution of equivalent strain was like the FEA results explained by Y.Q Wang. But the maximum strain at the face of the tube existed at the small portion only, thus concludes that the models are safe. The study of the deformation of the flange-plate could also be done by FEA and then compared with the test results. Since this is the theoretical study, FEA results could only be compared with the theoretical calculations and from the parametric study, it was found that FEA results were in good agreement with the theoretical results. Hence, it verifies the theoretical analysis of the proposed method.

CHAPTER 6

DISCUSSION OF RESULTS

6.1 General

The study of the behavior of the flange-plate connection and the forces on the bolts due to variable geometric arrangement and loads were studied in CHAPTER 4 and CHAPTER 5. The design procedure including the steps that were integrated from the current design methods is explained in detail in CHAPTER 3. In this chapter, the results from the proposed design method are compared with the current design methods and from FEA results, the proposed method is checked if its assumption and procedure is correct or not. For the comparison, different design examples with different geometry and parameters are selected, and the plate are designed following the current and the proposed design methods and checked if the proposed method is valid or not. The geometry and the application of loads in the structure in design examples are as in Figure 6, Figure 7 and Figure 5. The dimensions and details of bolts and tube are given. Also, applied loads are already defined. Using proposed method, maximum force due to applied loads, prying force, bolt force and the flange plate geometry are calculated.

6.2 Comparison Between Current Methods and Proposed Method

In this section, to demonstrate the success of the proposed unified design method, four designs, problems are solved by different approaches and compared with the proposed method.

6.2.1 Design Problem 1

Given Parameters:

For Tube:

External Diameter of tube, Dt = 6.614 in.

Thickness of tube, t = 0.394 in.

External radius of tube, r = 3.307 in.

Tube yield stress, f_{yt} = 40 ksi

For Bolts:

Grade: 8.8 M 24

Diameter of bolts, Db = 0.945 in.

Distance from bolt circle line to tube face, b = 1.266 in.

Edge distance, a = 1.266 in.

Number of bolts, n = 8

Design value of bolt tensile capacity, N_t^b = 45 kips

For Flange Plate:

Flange plate yield stress, f_{yf} = 60 ksi

Loads:

Bending Moment, M = 400 kips-in

Axial tensile load, N = 20 kips

Tensile capacity of each zone of tube, T = 45 kips/in

Solution:

Diameter of bolt circle, D_{bc} = 9.146 in.

Diameter of flange plate, D_f = 11.678 in.

a) Method 1, Y.Q Wang, 2013:

B_{eff} = Average length between yield lines = $\pi * \frac{9.146-6.614}{2*8}$ =3.093 in.

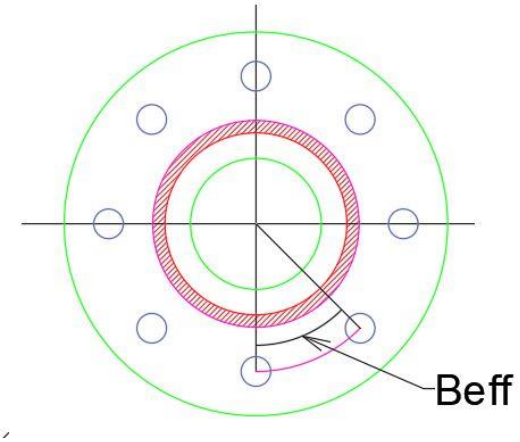

Figure 28. Calculation of Beff in method 1.

Maximum tensile force of bolts, $N_{max} = \frac{\pi*M}{n*D_{bc}} = \frac{\pi*400}{8*9.146} = 17.166\ kips < N_t^b \quad OK$

Tensile capacity index of one plate zone, $\gamma = n * \frac{r+b}{b} * \tan\left(\frac{\pi}{2n}\right)$

$$= 8 * \frac{3.307 + 1.266}{1.266} * \tan\left(\frac{\pi}{2 * 8}\right) = 5.745$$

First iterative flange plate thickness, $t_{f1} = \sqrt{\frac{6*T}{f_{yf}*\gamma}} = \sqrt{\frac{6*45}{60*5.745}} = 0.885\ in.$

Flange plate thickness with no prying,

$t_{fc} = \sqrt{\frac{4*N_t^b*b}{f_{yf}*B_{eff}}} = \sqrt{\frac{4*45*1.266}{60*3.093}} = 1.108\ in. \quad > t_{f1} \quad (OK)$ (The calculated thickness of plate should be less than the maximum thickness without prying action.)

Flange plate thickness when plate is in double curvature,

$t_{fd} = \sqrt{\frac{2*N_t^b*b}{f_{yf}*B_{eff}}} = \sqrt{\frac{2*45*1.266}{60*3.093}} = 0.784\ in.$

Flange plate thickness, t_{f2} = maximum (t_{f1}, t_{fd}) = 0.885 in.

Prying force, $Q = \frac{\alpha}{1+\alpha} * N_{max}$ $\qquad$ $Q = \frac{1}{1+1} * 17.166$

Q = 8.583 kips

Bolt Force, B = N_{max}+ Q = 25.749 kips < N_t^b $\qquad$ OK

Flange plate thickness, t_f = 0.885 in.

b) Method 2: TIA, 2014:

Anchor rod force correction factor, n_c = 1.27

Max. tensile force, $P_u = \frac{n_c*\pi*M}{n*D_{bc}} + \frac{N}{n} = \frac{1.27*\pi*400}{8*9.146} + \frac{20}{8} = 24.3\ kips$

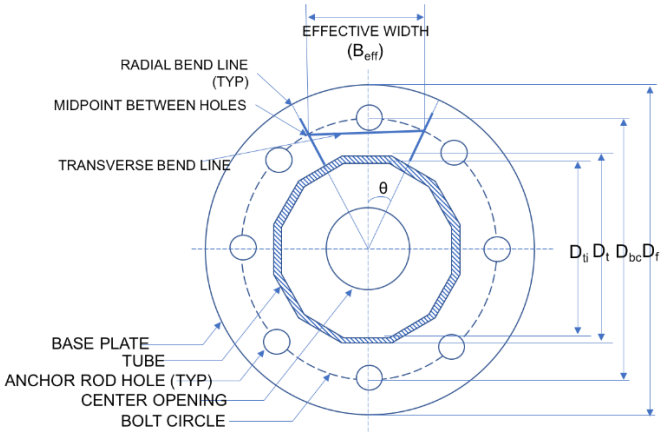

Figure 29. Calculation of Beff in method 2

b = 0.50* (D_{bc}-D_t) = 0.5*(9.146-6.614) = 1.266 in.

$\theta = minimum\ of\ (\theta_1, \theta_2\ and\ \theta_3)$

$\theta_1 = \frac{\pi}{n} = \frac{\pi}{8} = 0.3925\ rad$

$\theta_2 = \theta_1 = 0.3925\ rad$

$\theta_3 = cos^{-1}\left(\frac{D_{bc}+D_t}{2*D_{bc}}\right) = cos^{-1}\left(\frac{9.146+6.614}{2*9.146}\right) = 0.532\ rad$

$\theta = 0.3925\ rad$

Effective flange plate width resisting bending from radial bend lines,

$B_{er} = D_{bc}\sin(\theta) = 9.146 * \sin(0.3925) = 3.498\ in.$

Effective flange plate width resisting bending from transverse bend lines,

$B_{et} = (D_f - D_t)sin\theta = (11.78 - 6.614)\sin(0.3925) = 1.937\ in.$

Total effective flange plate width resisting bending, B_{eff} = 3.498+1.937 = 5.435 in

Flange Plate thickness,

$t_f = \sqrt{\frac{4*P_u*x}{0.9*f_{fy}*B_{eff}}} = \sqrt{\frac{4*24.3*1.266}{0.9*60*5.435}} = 0.648\ in.$

c) Proposed Method:

B_{eff} = Average length between yield lines = $\pi * \frac{9.146-6.614}{2*8} = 3.093$ in.

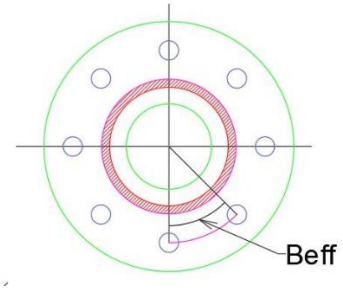

Figure 30. Calculation Beff in proposed method

Maximum tensile force of bolts, $N_{max} = \frac{\pi * M}{n * D_{bc}} + \frac{N}{n} = \frac{\pi * 400}{8 * 9.146} + \frac{20}{8} = 19.666\ kips$

Prying Force, $Q = \frac{1}{2} * N_{max} * \frac{1}{0.6} = \left(\frac{1}{2} * 19.666 * \frac{1}{0.6}\right) = 16.382\ kips$

Bolt Force, B = N_{max} + Q = 36.048 kips

Flange plate thickness,

$$t_f = \sqrt{\frac{4 * N_{max} * b}{0.9 * f_{fy} * B_{eff}}} = \sqrt{\frac{4 * 19.666 * 1.266}{0.9 * 60 * 3.093}} = 0.772\ in.$$

6.2.2 Design Problem 2

Given Parameters:

For Tube:

External Diameter of tube, Dt = 8.622 in.

Thickness of tube, t = 0.394 in.

External radius of tube, r = 4.311 in.

Tube yield stress, f_{yt} = 40 ksi

For Bolts:

Grade: 8.8 M 24

Diameter of bolts, Db = 0.945 in.

Distance from bolt circle line to tube face, b = 1.544 in.

Edge distance, a = 1.544 in.

Number of bolts, n = 12

Design value of bolt tensile capacity, N_t^b = 45 kips

For Flange Plate:

Flange plate yield stress, f_{yf} = 60 ksi

Loads:

Bending Moment, M = 600 kips-in

Axial tensile load, N = 40 kips

Tensile capacity of each zone of tube, T = 50 kips-in/in

Solution:

Diameter of bolt circle, D_{bc} = 11.71 in.

Diameter of flange plate, D_f = 14.798in.

a) Method 1, Y.Q Wang, 2013:

B_{eff} = Average length between yield lines = 2.660 in.

Maximum tensile force of bolts, $N_{max} = \frac{\pi * M}{n * D_{bc}} = \frac{\pi * 600}{12 * 11.71} = 13.40\ kips < N_t^b \quad OK$

Tensile capacity index of one plate zone, $\gamma = n * \frac{r+b}{b} * \tan\left(\frac{\pi}{2n}\right) = 5.988$

First iterative flange plate thickness, $t_{f1} = \sqrt{\frac{6*T}{f_{yf}*\gamma}} = \sqrt{\frac{6*50}{60*5.988}} = 0.914\ in.$

Flange plate thickness with no prying,

$t_{fc} = \sqrt{\frac{4*N_t^b*b}{f_{yf}*B_{eff}}} = \sqrt{\frac{4*45*1.544}{60*2.660}} = 1.320\ in. \quad > t_{f1} \quad (OK)$

Flange plate thickness when plate is in double curvature,

$t_{fd} = \sqrt{\frac{2*N_t^b*b}{f_{yf}*B_{eff}}} = \sqrt{\frac{2*45*1.544}{60*2.660}} = 0.933\ in.$

Flange plate thickness, t_{f2} = maximum (t_{f1}, t_{fd}) = 0.933 in.

Prying force, $Q = \frac{\alpha}{1+\alpha} * N_{max} \qquad Q = \frac{1}{1+1} * 13.40$

Q = 6.7 kips

Bolt Force, B = N_{max}+ Q = 20.1 kips < N_t^b OK

Flange plate thickness, t_f = 0.933 in.

b) Method 2: TIA, 2014:

Anchor rod force correction factor, n_c = 1.27

Max tensile force, $P_u = \frac{n_c * \pi * M}{n * D_{bc}} + \frac{N}{n} = \frac{1.27 * \pi * 600}{12 * 11.71} + \frac{40}{12} = 20.361\ kips$

Effective moment arm of bolt force, x = 0.50* (D_{bc}-D_t) = 1.544 in.

$\theta = minimum\ of (\theta_1, \theta_2\ and\ \theta_3)$

$\theta_1 = \frac{\pi}{n} = 0.262\ rad$

$\theta_2 = \theta_1 = 0.262\ rad$

$\theta_3 = cos^{-1}\left(\frac{D_{bc}+D_t}{2*D_{bc}}\right) = 0.519\ rad$

$\theta = 0.262\ rad$

Effective flange plate width resisting bending from radial bend lines,

$B_{er} = D_{bc} \sin(\theta) = 3.029\ in.$

Effective flange plate width resisting bending from transverse bend lines,

$B_{et} = (D_f - D_t) sin\theta = 1.598 in.$

Total effective flange plate width resisting bending, B_{eff} = 4.627 in

Flange Plate thickness,

$t_f = \sqrt{\frac{4 * P_u * x}{0.9 * f_{fy} * B_{eff}}} = \sqrt{\frac{4 * 20.361 * 1.544}{0.9 * 60 * 4.627}} = 0.709\ in.$

Flange plate thickness, t_f = 0.709 in.

c) Proposed Method:

B_{eff} = Average length between yield lines = 2.660 in.

Maximum tensile force of bolts, $N_{max} = \frac{\pi * M}{n * D_{bc}} + \frac{N}{n} = \frac{\pi * 600}{12 * 11.71} + \frac{40}{12} = 16.741\ kips$

Prying Force, $Q = \frac{1}{2} * N_{max} * \frac{1}{0.6} = \left(\frac{1}{2} * 16.741 * \frac{1}{0.6}\right) = 13.945\ kips$

Bolt Force, B = N_{max} + Q = 30.686 kips

Flange plate thickness,

$$t_f = \sqrt{\frac{4 * N_{max} * b}{0.9 * f_{fy} * B_{eff}}} = 0.848\ in.$$

6.2.3 Design Problem 3

Given Parameters:

For Tube:

External Diameter of tube, Dt = 16.242 in.

Thickness of tube, t = 0.394 in.

External radius of tube, r = 8.121 in.

Tube yield stress, f_{yt} = 40 ksi

For Bolts:

Grade: 8.8 M 24

Diameter of bolts, Db = 0.945 in.

Distance from bolt circle line to tube face, b = 1.826 in.

Edge distance, a = 1.826 in.

Number of bolts, n = 16

Design value of bolt tensile capacity, N_t^b = 45 kips

For Flange Plate:

Flange plate yield stress, f_{yf} = 60 ksi

Loads:

Bending Moment, M = 800 kips-in

Axial tensile load, N = 80 kips

Tensile capacity of each zone of tube, T = 52 kips-in/in

Solution:

Diameter of bolt circle, D_{bc} = 19.894 in.

Diameter of flange plate, D_f = 23.546 in.

a) Method 1, Y.Q Wang, 2013:

B_{eff} = Average length between yield lines = 3.546 in.

Maximum tensile force of bolts, $N_{max} = \frac{\pi * M}{n * D_{bc}} = \frac{\pi * 800}{16 * 19.894} = 7.892\ kips < N_t^b \quad OK$

Tensile capacity index of one plate zone, $\gamma = n * \frac{r+b}{b} * \tan\left(\frac{\pi}{2n}\right) = 8.580$

First iterative flange plate thickness, $t_{f1} = \sqrt{\frac{6*T}{f_{yf}*\gamma}} = \sqrt{\frac{6*52}{60*8.580}} = 0.778\ in.$

Flange plate thickness with no prying,

$t_{fc} = \sqrt{\frac{4*N_t^b*b}{f_{yf}*B_{eff}}} = 1.243\ in. \quad > t_{f1} \quad (OK)$

Flange plate thickness when plate is in double curvature,

$t_{fd} = \sqrt{\frac{2*N_t^b*b}{f_{yf}*B_{eff}}} = 0.879\ in.$

Flange plate thickness, t_{f2} = maximum (t_{f1}, t_{fd}) = 0.879 in.

Prying force, $Q = \frac{\alpha}{1+\alpha} * N_{max} \qquad Q = \frac{1}{1+1} * 7.892$

Q = 3.946 kips

Bolt Force, B = N_{max}+ Q = 11.839 kips < N_t^b OK

Flange plate thickness, t_f = 0.879 in.

b) Method 2: TIA, 2014:

Anchor rod force correction factor, n_c = 1.27

Max tensile force, $P_u = \frac{n_c * \pi * M}{n * D_{bc}} + \frac{N}{n} = \frac{1.27 * \pi * 800}{16 * 19.894} + \frac{80}{16} = 15.023\ kips$

Effective moment arm of bolt force, x = 0.50* (D_{bc}-D_t) = 1.826 in.

$\theta = minimum\ of\ (\theta_1, \theta_2\ and\ \theta_3)$

$\theta_1 = \frac{\pi}{n} = \frac{\pi}{16} = 0.196\ rad$

$\theta_2 = \theta_1 = 0.196\ rad$

$\theta_3 = cos^{-1}\left(\frac{D_{bc}+D_t}{2*D_{bc}}\right) = 0.432\ rad$

$\theta = 0.196\ rad$

Effective flange plate width resisting bending from radial bend lines,

$B_{er} = D_{bc} \sin(\theta) = 3.879\ in.$

Effective flange plate width resisting bending from transverse bend lines,

$B_{et} = (D_f - D_t) sin\theta = 1.424\ in.$

Total effective flange plate width resisting bending, B_{eff} = 5.303 in

Flange Plate thickness,

$t_f = \sqrt{\frac{4 * P_u * x}{0.9 * f_{fy} * B_{eff}}} = \sqrt{\frac{4 * 15.023 * 1.826}{0.9 * 60 * 5.303}} = 0.619\ in.$

Flange plate thickness, t_f = 0.619 in.

c) Proposed Method:

B_{eff} = Average length between yield lines = 3.546 in.

Maximum tensile force of bolts, $N_{max} = \frac{\pi * M}{n * D_{bc}} + \frac{N}{n} = \frac{\pi * 800}{16 * 19.894} + \frac{80}{16} = 12.892\ kips$

Prying Force, $Q = \frac{1}{2} * N_{max} * \frac{1}{0.6} = \left(\frac{1}{2} * 12.892 * \frac{1}{0.6}\right) = 10.739\ kips$

Bolt Force, B = N_{max} + Q = 23.631 kips

Flange plate thickness,

$$t_f = \sqrt{\frac{4 * N_{max} * b}{0.9 * f_{fy} * B_{eff}}} = \sqrt{\frac{4 * 23.631 * 1.826}{0.9 * 60 * 3.546}} = 0.701\ in.$$

6.2.4 Design Problem 4

Given Parameters:

For Tube:

External Diameter of tube, Dt = 20.002 in.

Thickness of tube, t = 0.394 in.

External radius of tube, r = 10.001 in.

Tube yield stress, f_{yt} = 40 ksi

For Bolts:

Grade: 8.8 M 24

Diameter of bolts, Db = 0.945 in.

Distance from bolt circle line to tube face, b = 1.924 in.

Edge distance, a = 1.924 in.

Number of bolts, n = 20

Design value of bolt tensile capacity, N_t^b = 45 kips

For Flange Plate:

Flange plate yield stress, f_{yf} = 60 ksi

Loads:

Bending Moment, M = 1200 kips-in

Axial tensile load, N = 140 kips

Tensile capacity of each zone of tube, T = 60 kips-in/in

Solution:

Diameter of bolt circle, D_{bc} = 23.85 in.

Diameter of flange plate, D_f = 27.698 in.

a) Method 1, Y.Q Wang, 2013:

B_{eff} = Average length between yield lines = 3.442 in.

Maximum tensile force of bolts, $N_{max} = \frac{\pi * M}{n * D_{bc}} = \frac{\pi * 140}{20 * 23.85} = 7.899\ kips < N_t^b \quad OK$

Tensile capacity index of one plate zone, $\gamma = n * \frac{r+b}{b} * \tan\left(\frac{\pi}{2n}\right) = 9.751$

First iterative flange plate thickness, $t_{f1} = \sqrt{\frac{6*T}{f_{yf}*\gamma}} = \sqrt{\frac{6*60}{60*9.751}} = 0.784\ in.$

Flange plate thickness with no prying,

$$t_{fc} = \sqrt{\frac{4*N_t^b*b}{f_{yf}*B_{eff}}} = 1.295\ in. \quad > t_{f1} \quad (OK)$$

Flange plate thickness when plate is in double curvature,

$$t_{fd} = \sqrt{\frac{2*N_t^b*b}{f_{yf}*B_{eff}}} = 0.916\ in.$$

Flange plate thickness, $t_{f\,2}$= maximum (t_{f1}, t_{fd}) = 0.916 in.

Prying force, $Q = \frac{\alpha}{1+\alpha} * N_{max} \qquad Q = \frac{1}{1+1} * 7.899$

Q = 3.95kips

Bolt Force, B = N_{max}+ Q = 11.848 kips < N_t^b OK

Flange plate thickness, t_f = 0.916 in.

b) Method 2: TIA, 2014:

Anchor rod force correction factor, n_c = 1.27

Max tensile force, $P_u = \frac{n_c * \pi * M}{n * D_{bc}} + \frac{N}{n} = \frac{1.27 * \pi * 1200}{20 * 23.85} + \frac{140}{20} = 17.032\ kips$

Effective moment arm of bolt force, x = 0.50* (D_{bc}-D_t) = 1.924 in.

$\theta = minimum\ of (\theta_1, \theta_2\ and\ \theta_3)$

$\theta_1 = \frac{\pi}{n} = \frac{\pi}{8} = 0.157\ rad$

$\theta_2 = \theta_1 = 0.157\ rad$

$\theta_3 = cos^{-1}\left(\frac{D_{bc} + D_t}{2 * D_{bc}}\right) = 0.404\ rad$

$\theta = 0.157\ rad$

Effective flange plate width resisting bending from radial bend lines,

$B_{er} = D_{bc} \sin(\theta) = 3.729\ in.$

Effective flange plate width resisting bending from transverse bend lines,

$B_{et} = (D_f - D_t) sin\theta = 1.203\ in.$

Total effective flange plate width resisting bending, B_{eff} = 4.932 in

Flange Plate thickness,

$t_f = \sqrt{\frac{4 * P_u * x}{0.9 * f_{fy} * B_{eff}}} = \sqrt{\frac{4 * 17.032 * 1.924}{0.9 * 60 * 4.932}} = 0.702\ in.$

Flange plate thickness, t_f = 0.702 in.

c) Proposed Method:

From Drawing:

B_{eff} = Average length between yield lines = 3.152 in.

Maximum tensile force of bolts, $N_{max} = \frac{\pi * M}{n * D_{bc}} + \frac{N}{n} = \frac{\pi * 1200}{20 * 23.85} + \frac{140}{20} = 14.899\ kips$

Prying Force, $Q = \frac{1}{2} * N_{max} * \frac{1}{0.6} = \left(\frac{1}{2} * 14.899 * \frac{1}{0.6}\right) = 12.411\ kips$

Bolt Force, $B = N_{max} + Q = 27.311$ kips

Flange plate thickness,

$$t_f = \sqrt{\frac{4 * N_{max} * b}{0.9 * f_{fy} * B_{eff}}} = \sqrt{\frac{4 * 14.899 * 1.924}{0.9 * 60 * 3.442}} = 0.785\ in.$$

6.2.5 Comparison

With the results from above four design examples, the comparison of results calculated from three different methods were plotted in Figure 31, Figure 32 and Figure 33.

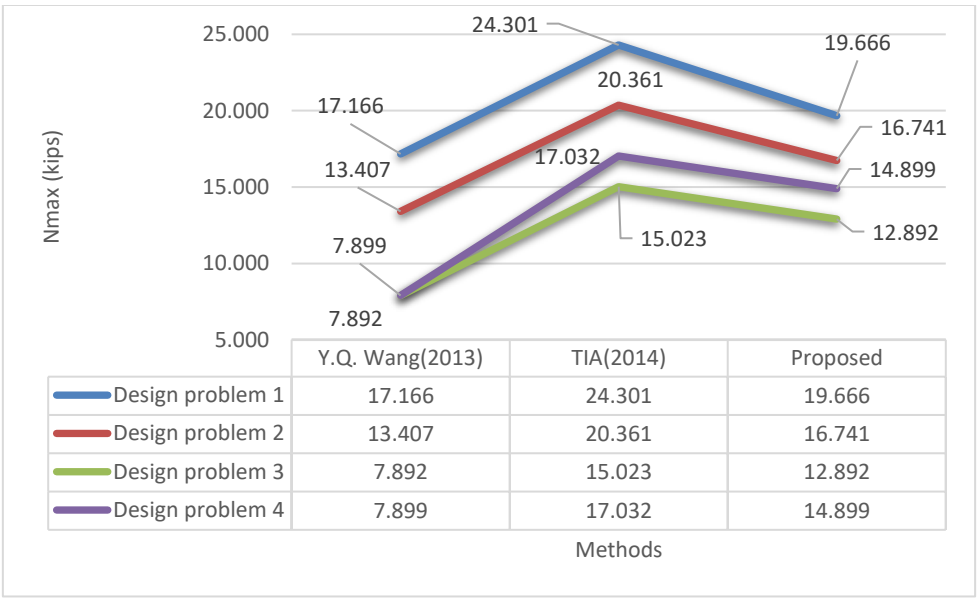

Figure 31. Comparison of maximum tensile force of bolts from three methods

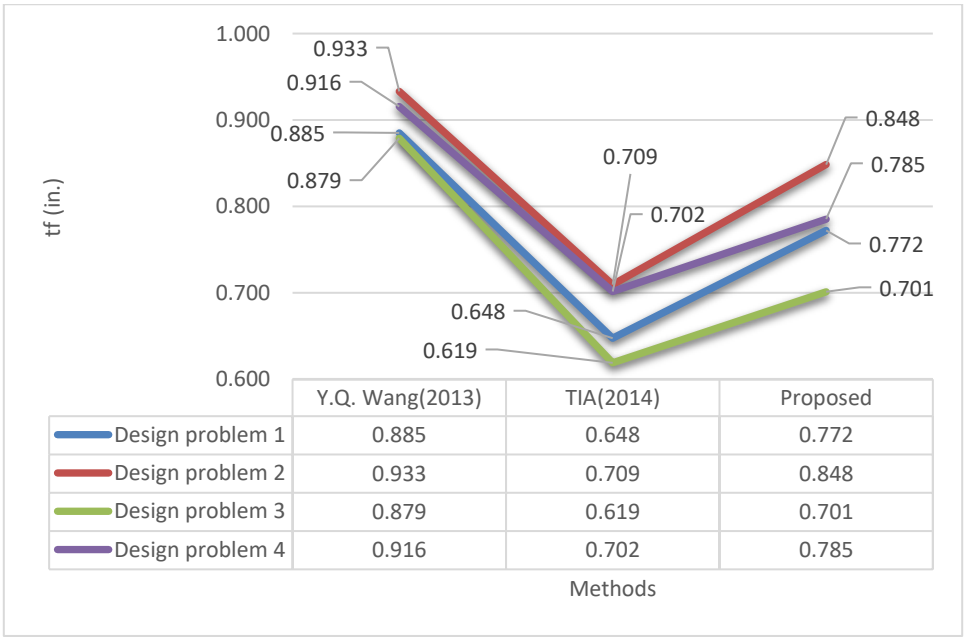

Figure 32. Comparison of flange-plate thickness calculated from three methods

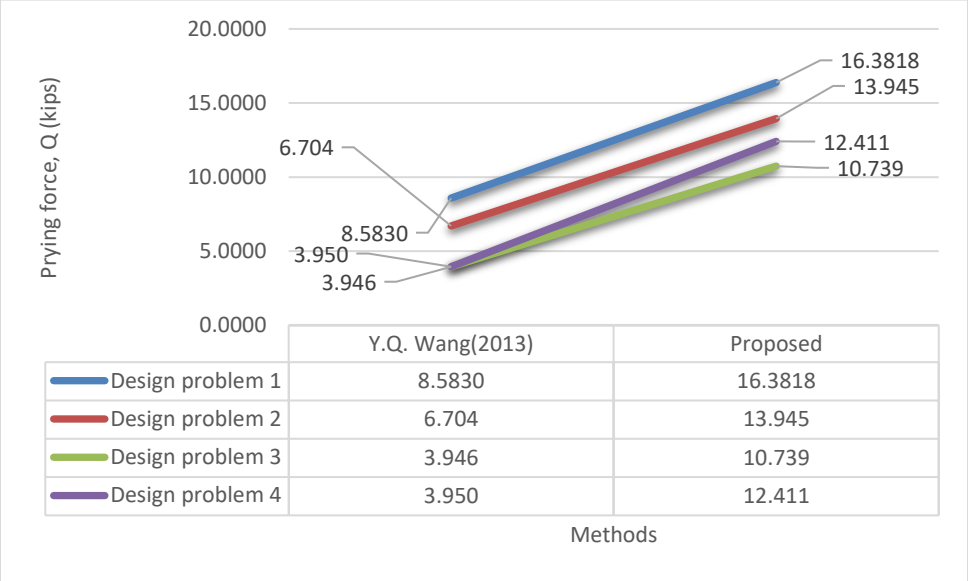

Figure 33. Comparison of prying force calculated from two methods

In Figure 31, the variation of maximum tensile force of bolts using three methods can be seen. The calculation using Y.Q Wang (2013)'s method gave less value of N_{max} because it was based on the bending moment only. There was no tensile force in his study. Whereas, N_{max} using TIA (2014) gives higher value since it included bolt correction factor, n_c in the design. In the proposed design method, the results were seen considering bending moment and axial tensile force and neglecting n_c. Thus, the result in Figure 32 showed values for the proposed method that lies in between the other two methods.

Figure 32 represented the flange-plate thickness results using three methods. The thickness from Y.Q Wang, 2013 was greater than other two methods. The calculation of the flange-plate thickness in that method considered the bending of the tube and other

two methods considered the maximum tensile force of the bolts. The TIA method assumed transverse and radial yield lines and the effective width of bending considering these two yield lines was greater than the effective width of bending in the proposed method that assumed two radial yield lines.

The results showing the difference in the prying force between two methods were shown in Figure 33. The calculation of prying force in the proposed method was based on the experimental verification and the FEA confirmation done in the paper by F. Huang (2017). There is a big difference in the prying force between two methods, which describes that for unstiffened connections, method 1 was under designed.

6.3 Comparison Between Proposed Method and FEA Results

The numerical verification of the proposed method was supported by FEA using ANSYS R18.0. The parametric study results from FEA showed similar results as the theoretical calculation. The parametric study with FEA was explained in CHAPTER 5. Furthermore, with the applied load and bending moment, maximum stress could be seen in the tensile face of the tube. This was similar with the failure case, where the failure of unstiffened connection for CHS occurred when the full penetration welds between the tube and the flange plates fractured (Y.Q Wang et al, 2013). Besides verifying the assumptions, the normal stress at the bolts from the theoretical calculation using the proposed method and the FEA were compared in Table 7. The two models are the design examples 1 and 2 of this chapter. This comparison of theoretical normal stress and FEA stress provided another tool of verification. The comparison ratio between the theoretical calculation and FEA results showed that the FEA results were in good agreement with the theoretical calculation results.

The theoretical calculation for normal stress at the bolts are:

$\sigma = \frac{N_{max}}{A}$, σ = normal stress, N_{max} = maximum tensile force on bolts, A = area of bolts

For Model 1, N_{max} = 19666 lbs, A = 0.70138 in^2

$$\sigma = \frac{19666}{0.70138} = 28039\ psi$$

For B1-2, N_{max} = 16741 lbs, A = 0.70138 in^2

$$\sigma = \frac{16741}{0.70138} = 23868\ psi$$

Table 7. Comparison of normal stress at plate critical section

Design Example	Proposed method (psi)	FEA (psi)	Proposed Method / FEA
1	28039	29526	0.95
2	23868	25714	0.93

CHAPTER 7

SUMMARY AND RECOMMENDATIONS

7.1 Summary

This is a theoretical study that aims to come up with simplified unified design method for circular bolted flange plate connections. To achieve this goal, the literature review of articles and papers were done, and few papers were selected. Integrating the steps, and elimination of the limitations of the selected methods were done to propose simplified design steps. The proposed method is applicable for the unstiffened steel circular bolted flange plate connections for minimum of 8 bolts. For this study, the geometry and properties of bolts and tube were defined, applied loads were defined. With these information, the maximum loads due to applied loads, the prying force, the total bolt force and the flange-plate thickness were calculated. A parametric study including variable parameters and the calculations following the design steps of the proposed method are explained in CHAPTER 4. FEA using ANSYS R18.0 supported and verified the results of the proposed method. Moreover, few examples were selected, and the flange-plate connections were designed using two literature methods and the proposed method. The results from these methods were compared, and the proposed method results showed that it was more appropriate than the current literature methods. The comparison and the FEA results verified that the proposed method was valid and could be used in the design of unstiffened circular bolted flange plate connections.

7.2 Limitations of the proposed method

This research was focused on the design of bolted flange connections. There are few limitations of the use of proposed method in this study.

1) The proposed method considered bending moment and axial tensile force in the calculation. Consideration of axial compression and shear forces were neglected.
2) This method was applicable for number of bolts equal to 8 or greater than 8. This did not explain the equations for number of bolts less than 8.
3) In the derivation and calculations, the distance a and b were assumed to be equal. This method did not study the case for different value of a and b.

7.3 Recommendations for Future Research

This study was limited to steel circular bolted flange plates. Additional future is recommended to include the following:

1) Experimental verification of the proposed method developed by our research. Hence, laboratory experiments with the variable geometry of the tube, number of bolts, and flange-plate with variable loads could be carried out and the results like deformation and strain can be compared with the FEA results.
2) This study mainly focused on the unstiffened flange-plate. Further study for the stiffened flange plate connections can be carried out and it can be again verified with the experimental and analytical results.
3) In this study a unified design method for flange plates connecting steel to steel members was proposed. Flange plates connecting steel to concrete members

or concrete to concrete members were not investigated due to time constraints. Thus, future research should investigate the applicability of the proposed method to these types of connections and identify any modifications that may be needcd.

REFERENCES

1. Cao JJ, Packer JA, Yang GJ. (1998). Yield line analysis of RHS connections with axial loads. *Construction Steel Research*, 48(1):1-25.
2. Fenghua Huang, Dachang Zhang, Wan Hong, Buhuli Li. (2017). Mechanism and calculation theory of prying force for flexible flange connection. *Construction Steel Research*, 132:97-107.
3. G M PinFold. (1994). Effect of flange geometry on the strength of bolted joint. *CICIND's 42nd meeting*, Vol. 11, No. 2.
4. H.Z. Deng, Y. Huang, X.H. Jin. (2009). *Experimental research on large-scale flange joints of steel.* London, UK: 2009 Taylor & Francis Group.
5. Henk Van Koten. (n.d.). Steel Chimney Design. In *CICIND* (pp. 167-220).
6. Igarashi S, Wakiyama K, Inoue K, Matsumoto T, Murase Y. (1985). Limit design of high strength bolted tube flange joints Part 1. *Architectural Institute of Japan* (pp. 52-66). Tokyo: A.I.J.
7. Igarashi S, Wakiyama K, Inoue K, Matsumoto T, Murase Y. (1985). Limit design of high strength bolted tube flange joints Part 2. *Architectural Institute of Japan* (pp. 71-82). Tokyo: A.I.J.
8. Kato B, Hirose R. (1985). Bolted tension flanges joining circular hollow section members. *Construction Steel Res*, 5(2):79101.
9. Kato B, Mukai A. (1985). Bolted tension flanges joining square hollow section members. *Construction Steel Research*, 5(3):163-77.

10. Louis F. Geschwindner. (2008). *Unified Design of Steel Structures.* Pennsylvania: John Wiley & Sons.
11. Mael Cauchaux, Mohammed Hijaj, Ivor Ryan, Alain Bureau. (2011). Bolted circular flange connections; Bending and axial static resistances. *Eurosteel.* Budapest: Eurosteel.
12. Packer JA, Bruno L, Pirkemoe PC. (1989). Limit analysis of bolted RHS flange plate joints. *Structural Engineering*, 115(9):2226-42.
13. *Steel Construction Manual.* (Thirteenth Edition). American Institute of Steel Construction.
14. TIA. (2014, December). Structural Standards for Steel Antenna Towers and Antenna Supporting Structures-Addendum 3. *ANSI*. Arlington, Virginia, U.S.A.: Telecommunications Industry Association.
15. Willibald S, Packer JA, Puthli RS. (2003). Design recommendations for bolted rectangular HSS flange-plate connection in axial tension. *Engineering*, 40(1):15-24.
16. Y.Q. Wang, L. Zong, Y.J. Shi. (2013). Bending behavior and design model of bolted flange-plate connection. *Construction Steel Research*, 84:1-16.

APPENDIX A

EXCEL CALCULATION

The calculations for the proposed method was done in the excel sheet. In the calculation, there was the input part, and the design calculation part. Firstly, the geometry and material of bolts and tube are defined and tabulated as shown below.

Bolts Parameters

S.N	Grade	Dia of bolts, Db (in.)	b (in.)	a (in.)	no. of bolts, n	$N_t^b\,(kips)$
1	8.8M24	0.945	1.266	1.266	8	45
2	8.8M24	0.945	1.544	1.544	12	45
3	8.8M24	0.945	1.826	1.826	16	45
4	8.8M24	0.945	1.924	1.924	20	45

Tube Parameters

S.N	Dt (in.)	r (in.)	t (in.)	fyt (ksi)	axial load, N (kips)	Bending moment, M (kips-in)
1	6.614	3.307	0.394	40	20	400
2	8.622	4.311	0.394	40	40	600
3	16.242	8.121	0.394	40	80	800
4	20.002	10.001	0.394	40	140	1200

Then, using the external tube diameter, and value of b and a, external flange plate diameter was defined. After that, internal diameter of flange plate assuming it should be less than the internal diameter of tube was defined. The flange plate geometry and material property are shown below.

Flange Plate Parameters

S.N	Df (in.)	df(in.)	fyf (ksi)
1	11.678	2.22	60
2	14.798	4.228	60
3	23.546	11.848	60
4	27.698	15.608	60

Using these data, the design calculations are done for all four cases. The design calculations include, maximum loads due to applied loads, prying force, total bolt force and the flange-plate thickness.

Design Calculations

S.N	Dia of bolt circle, Dbc (in.)	Nmax (kips)	Q (kips)	B (kips)	Check	Beff (in.)	tf (in.)
1	9.146	19.666	16.382	36.048	OK	3.093	0.772
2	11.71	16.741	13.945	30.686	OK	2.660	0.848
3	19.894	12.892	10.739	23.631	OK	3.546	0.701
4	23.85	14.899	12.411	27.311	OK	3.442	0.785